Supersymmetric *R*-parity violating Dine-Fischler-Srednicki-Zhitnitsky axion model

Stefano Colucci,[1,*] Herbi K. Dreiner,[1,†] and Lorenzo Ubaldi[2,3,‡]

[1]*Physikalisches Institut der Universität Bonn, Bethe Center for Theoretical Physics, Nußallee 12, 53115 Bonn, Germany*
[2]*SISSA International School for Advanced Studies, Via Bonomea 265, 34136 Trieste, Italy*
[3]*INFN - Sezione di Trieste, Via Bonomea 265, 34136 Trieste, Italy*

We propose a complete *R*-parity violating supersymmetric model with baryon triality that contains a Dine-Fischler-Srednicki-Zhitnitsky axion chiral superfield. We parametrize supersymmetry breaking with soft terms and determine under which conditions the model is cosmologically viable. As expected we always find a region of parameter space in which the axion is a cold dark matter candidate. The mass of the axino, the fermionic partner of the axion, is controlled by a Yukawa coupling. When heavy [$\mathcal{O}(\text{TeV})$], the axino decays early and poses no cosmological problems. When light [$\mathcal{O}(\text{keV})$], it can be long lived and a warm dark matter candidate. We concentrate on the latter case and study in detail the decay modes of the axino. We find that constraints from astrophysical x rays and gamma rays on the decay into photon and neutrino can set new bounds on some trilinear supersymmetric *R*-parity violating Yukawa couplings. In some corners of the parameter space the decays of a relic axino can also explain a putative 3.5 keV line.

I. INTRODUCTION

Supersymmetry (SUSY) is the best candidate to explain the hierarchy problem of the Standard Model (SM) [1,2], and thus a leading candidate for the discovery of new physics effects at the LHC. Most supersymmetric models which have been searched for at the LHC make the assumption of conserved *R*-parity [3]. A very restrictive and widely considered version with universal boundary conditions at the unification scale, the constrained minimal supersymmetric Standard Model (CMSSM) [4] is now in considerable tension with collider data [5]. The *R*-parity violating (RpV) CMSSM is still very much allowed [6].

R-parity is a discrete multiplicative symmetry invoked in the CMSSM to forbid baryon and lepton number violating operators which together lead to rapid proton decay. The bonus of imposing *R*-parity is that the lightest supersymmetric particle (LSP), typically the neutralino, is stable

and provides a dark matter (DM) candidate in the form of a weakly interacting massive particle (WIMP). This is the most popular and most searched for DM candidate. However, to date no neutralino dark matter has been found [7–9]. It is thus prudent to investigate other DM candidates, also within alternative supersymmetric models.

R-parity does not forbid some dimension-five operators dangerous for proton decay [10]. This issue can be resolved by imposing a Z_6 discrete symmetry, known as proton hexality (P_6), which leads to the same renormalizable superpotential as *R*-parity [11,12], but is incompatible with a grand unified theory symmetry. Alternatively, one can impose a Z_3 symmetry known as baryon-triality (B_3) [11,13–18]. The latter allows for lepton number violating operators in the superpotential thanks to which the neutrinos acquire Majorana masses, without introducing a new very high energy Majorana mass scale [15–17,19–24]. This is a virtue of B_3 models.[1] A possible handicap is that the LSP is unstable and is not a dark matter candidate. This can be naturally resolved when taking into account the strong *CP* problem, as we discuss in the following.

Besides the hierarchy problem, every complete model should also address the strong *CP* problem [30], which

*[*]colucci@th.physik.uni-bonn.de
[†]dreiner@th.physik.uni-bonn.de
[‡]ubaldi.physics@gmail.com

---

[1]Other than P_6 and B_3, one can also consider *R*-symmetries to restrict the renormalizable Lagrangian resulting in *R*-parity conservation or violation [25–29]. For our purposes this is equivalent.

plagues the SM, as well as its supersymmetric generalizations. In its simplest forms this necessitates introducing the pseudoscalar axion field [31,32]. In the supersymmetric versions, the axion is part of a chiral supermultiplet and is accompanied by another scalar, the saxion, and a spin-$1/2$ fermion, the axino.

In this paper we propose to study a B_3 model with the inclusion of an axion supermultiplet of the Dine-Fischler-Srednicki-Zhitnitsky (DFSZ) type [33,34]. The axion contributes to the DM energy density in the form of cold DM [35–38]. Depending on the value of its decay constant, f_a, it constitutes all or a fraction of the DM. The gravitino is heavy [$\mathcal{O}(\text{TeV})$], decays early in the history of the universe, and does not pose cosmological problems. The axino mass is proportional to $\lambda_\chi v_\chi$ [see Eq. (2.18)], where v_χ is the vacuum expectation value (VEV) of a scalar field of the order of the soft masses [$\mathcal{O}(\text{TeV})$], and λ_χ is a dimensionless Yukawa coupling in the superpotential. We consider two cases: (i) a heavy axino ($\sim$TeV, which requires $\lambda_\chi \sim 1$), and (ii) a light one ($\sim$keV, requiring $\lambda_\chi \ll 1$). In case (i) the axino decays early and is not a DM candidate. In the more interesting case (ii), it is the LSP, its lifetime is longer than the age of the universe, and it contributes as warm DM [39]. We study in detail its three decay channels: into an axion and a neutrino, into three neutrinos, and into a neutrino and a photon, the last one subject to constraints from x- and gamma-ray data.

In 2014 a potential anomaly was observed in x-ray data coming from various galaxy clusters and the Andromeda galaxy [40,41]. There have been several papers discussing this in terms of an axino in R-parity violating supersymmetry [42–44], although we were able to show that this explanation is not probable [45].

The outline of the paper is as follows. In Sec. II, we introduce the model and describe its parameters and mass spectrum. In Sec. III we compute in detail the axino decay rates and branching fractions. In Sec. IV we consider cosmological and astrophysical constraints on the model, with a focus on the more interesting case of a light axino. We conclude with a discussion of our results and point out possible future directions of investigation.

In Appendix A we include some general comments on the axino mass, we discuss its dependence on the SUSY breaking scale, and we point out that DFSZ models accommodate more easily a light axino, as opposed to models *à la* Kim-Shifman-Vainshtein-Zakharov (KSVZ) [46,47]. In Appendix B we furthermore give details on the derivation of the mixings of the axino mass eigenstates.

II. THE RpV DFSZ SUPERSYMMETRIC AXION MODEL

A. The Lagrangian

The building blocks of the minimal supersymmetric DSFZ axion model are the particle content of the minimal supersymmetric Standard Model (MSSM) plus three superfields, which are necessary to construct a self-consistent axion sector as discussed in Ref. [48]. The particle content, the quantum numbers with respect to the SM gauge sector $SU(3)_c \times SU(2)_L \times U(1)_Y$, and the charges under the global Peccei-Quinn (PQ) symmetry [49], $U(1)_{\text{PQ}}$, are summarized in Table I. The renormalizable superpotential is given by

$$W = W_{B_3} + W_I + W_{\text{PQ}}, \qquad (2.1)$$

$$W_{B_3} = Y_u \hat{Q} \hat{H}_u \hat{\bar{U}} + Y_d \hat{Q} \hat{H}_d \hat{\bar{D}} + Y_e \hat{L} \hat{H}_d \hat{\bar{E}} + \frac{1}{2} \lambda \hat{L} \, \hat{L} \, \hat{\bar{E}}$$
$$+ \lambda' \hat{L} \, \hat{Q} \, \hat{\bar{D}}, \qquad (2.2)$$

$$W_I = c_1 \hat{A} \hat{H}_u \hat{H}_d + c_2 \hat{A} \, \hat{L} \, \hat{H}_u, \qquad (2.3)$$

$$W_{\text{PQ}} = \lambda_\chi \hat{\chi} \left(\hat{A} \, \hat{\bar{A}} - \frac{1}{4} f_a^2 \right). \qquad (2.4)$$

Here and in the following we suppress generation, as well as isospin and color indices. Superfields are denoted by a hat superscript. We have imposed the discrete Z_3 symmetry [11] known as baryon triality, B_3. This leaves only the RpV operators $\frac{1}{2} \lambda \hat{L} \, \hat{L} \, \hat{\bar{E}}$, $\lambda' \hat{L} \, \hat{Q} \, \hat{\bar{D}}$, and $c_2 \hat{A} \, \hat{L} \, \hat{H}_u$. We have generalized the usual bilinear operators $\mu H_u H_d$ and $\kappa_i L_i H_u$ to obtain PQ invariance. The PQ charges satisfy

$$Q_A + Q_{H_u} + Q_{H_d} = 0, \qquad Q_A + Q_{H_u} + Q_L = 0, \quad (2.5)$$

TABLE I. Charge assignments for the chiral superfields. Note in our R-parity violating supersymmetric models $Q_{H_d} = Q_L$.

Superfield	$SU(3)_C$	$SU(2)_L$	$U(1)_Y$	$U(1)_{\text{PQ}}$
$\hat{Q}$	3	2	$1/6$	Q_Q
$\hat{\bar{U}}$	$\bar{3}$	1	$-2/3$	$Q_{\bar{U}}$
$\hat{\bar{D}}$	$\bar{3}$	1	$1/3$	$Q_{\bar{D}}$
$\hat{L}$	1	2	$-1/2$	Q_L
$\hat{\bar{E}}$	1	1	1	$Q_{\bar{E}}$
$\hat{H}_d$	1	2	$-1/2$	Q_{H_d}
$\hat{H}_u$	1	2	$1/2$	Q_{H_u}
$\hat{A}$	1	1	0	Q_A
$\hat{\bar{A}}$	1	1	0	$-Q_A$
$\hat{\chi}$	1	1	0	0

from the terms in Eq. (2.3), and similar relations for the other fields that are readily obtained from the terms in the rest of the superpotential.

The PQ symmetry is spontaneously broken at the scale f_a, due to the scalar potential resulting from W_{PQ}, and the scalar parts of $\hat{A}$ and $\hat{\bar{A}}$ get VEVs v_A and $v_{\bar{A}}$, respectively,

$$A = \frac{1}{\sqrt{2}}(\phi_A + i\sigma_A + v_A), \qquad \bar{A} = \frac{1}{\sqrt{2}}(\phi_{\bar{A}} + i\sigma_{\bar{A}} + v_{\bar{A}}).$$
$$(2.6)$$

The VEVs must fulfill

$$v_A \cdot v_{\bar{A}} = \frac{1}{2}f_a^2, \qquad (2.7)$$

and we denote their ratio as

$$\tan^2\beta' \equiv \frac{v_{\bar{A}}}{v_A}. \qquad (2.8)$$

Below the PQ breaking scale, we generate an effective μ-term, $\mu_{\mathrm{eff}}\hat{H}_u\hat{H}_d$, and effective bilinear RpV κ-terms, $\kappa_{\mathrm{eff},i}\hat{L}_i\hat{H}_u$, with

$$\mu_{\mathrm{eff}} = \frac{c_1}{\sqrt{2}}v_A,$$
$$\kappa_{\mathrm{eff},i} = \frac{c_{2,i}}{\sqrt{2}}v_A. \qquad (2.9)$$

For successful spontaneous breaking of the electroweak (EW) symmetry, μ_{eff} should be of the order of the EW scale, while κ_{eff} is constrained by neutrino physics, as discussed below, and should be $\leq O(\mathrm{MeV})$. Since $f_a > 10^9$ GeV from astrophysical bounds on axions [50], the couplings c_1 and c_2 must be very small, roughly $c_1 < 10^{-6}$ and $c_2 < 10^{-11}$. They are, nonetheless, radiatively stable.

We have assumed that W_{PQ} respects an *R*-symmetry, under which the field $\hat{\chi}$ has charge 2. This forbids the superpotential terms $\hat{\chi}^2$ and $\hat{\chi}^3$. See also Ref. [25].

The soft-supersymmetric terms of this model consist of scalar squared masses, gaugino masses, and the counterparts of the superpotential couplings. The full soft Lagrangian reads

$$-\mathcal{L}_{\mathrm{soft}} = (M_1\tilde{B}\tilde{B} + M_2\tilde{W}\tilde{W} + M_3\tilde{g}\tilde{g} + \mathrm{H.c.}) + \tilde{f}^\dagger m_{\tilde{f}}^2\tilde{f} + m_\chi^2|\chi|^2 + m_A^2|A|^2 + m_{\bar{A}}^2|\bar{A}|^2 + m_{H_u}^2|H_u|^2 + m_{H_d}^2|H_d|^2$$
$$+ m_{\tilde{\ell}H_u}^2(\tilde{\ell}^\dagger H_u + H_u^\dagger\tilde{\ell}) + (B\mu H_d \cdot H_u + \mathrm{H.c.}) + (T_u\tilde{u}\,\tilde{q}\,H_u + T_d\tilde{d}\,\tilde{q}\,H_d + T_e\tilde{e}\,\tilde{\ell}\,H_d + T_\lambda\tilde{\ell}\,\tilde{\ell}\,\tilde{e}$$
$$+ T_{\lambda'}\tilde{\ell}\,\tilde{q}\,\tilde{d} + T_{c1}AH_uH_d + T_{c2}A\tilde{\ell}H_u + T_{\lambda_\chi}\chi A\bar{A} + L_V\chi + \mathrm{H.c.}), \qquad (2.10)$$

with $\tilde{f} \in \{\tilde{e}, \tilde{\ell}, \tilde{d}, \tilde{u}, \tilde{q}\}$. We assume that SUSY breaking violates the *R*-symmetry of the axion sector; hence we include the soft terms $T_{\lambda_\chi}\chi A\bar{A}$ and $L_V\chi$. Note that, even if set to zero at some scale, these terms would be generated at the two-loop level because of the small coupling to the MSSM sector, where no *R*-symmetry is present.

At low energy the Lagrangian contains interactions of the axion with the gauge fields. These are best understood by performing a field rotation[2] that leads to a basis in which all the matter fields are invariant under a PQ transformation [52]. We have

$$\mathcal{L}_{aVV} = \frac{a}{32\pi^2 f_a}(g_1^2 C_{aBB}B_{\mu\nu}\tilde{B}^{\mu\nu} + g_2^2 C_{aWW}W_{\mu\nu}^a\tilde{W}^{a\mu\nu}$$
$$+ g_3^2 G_{\mu\nu}^\alpha\tilde{G}^{\alpha\mu\nu}). \qquad (2.11)$$

Here a is the axion field which in our model is given by $a \simeq \frac{1}{\sqrt{2}}(\sigma_A - \sigma_{\bar{A}})$ to a good approximation[3]; cf. Eq. (2.6). $B_{\mu\nu}, W_{\mu\nu}^a, G_{\mu\nu}^a$ are the SM field strength tensors, here a is an

adjoint gauge group index, with $\tilde{X}^{a\mu\nu} \equiv \epsilon^{\mu\nu\rho\sigma}X_{\rho\sigma}^a$, and the coefficients are given in terms of the PQ charges

$$C_{aBB} = 3(3Q_Q + Q_L) - 7Q_A, \qquad (2.12)$$

$$C_{aWW} = -3(3Q_Q + Q_L) + Q_A. \qquad (2.13)$$

In the supersymmetric limit the couplings of the axino to gauginos and gauge fields are related to those in Eq. (2.11). We are, however, interested in the case of broken SUSY. In general, such axino couplings can be calculated explicitly, by computing triangle loop diagrams, once the full Lagrangian is specified, as it is in our model. Later in the paper we use the full Lagrangian to compute the one-loop decay of the axino into a photon and a neutrino, including the couplings.

B. The mass spectrum

We now turn our attention to the spin-$1/2$ neutral fermion mass spectrum of this model. The 10×10 mass matrix in the basis $(\lambda_{\tilde{B}}, \tilde{W}^0, \tilde{H}_u^0, \tilde{H}_d^0, \nu_{L,i}, \tilde{A}, \tilde{\bar{A}}, \tilde{\chi})$, which is a generalization of the MSSM neutralino mass matrix, reads

---

[2]See, for example, Appendix C of Ref. [51] for details.
[3]The axion also has a small admixture of H_u and H_d which we neglect here.

$$\mathcal{M}_{\chi^0} = \begin{bmatrix} M_1 & 0 & \frac{g_1 v_u}{2} & -\frac{g_1 v_d}{2} & 0 & 0 & 0 & 0 & 0 & 0 \\ 0 & M_2 & -\frac{g_2 v_u}{2} & \frac{g_2 v_d}{2} & 0 & 0 & 0 & 0 & 0 & 0 \\ \frac{g_1 v_u}{2} & -\frac{g_2 v_u}{2} & 0 & -\frac{c_1 v_A}{\sqrt{2}} & \frac{c_{2,1} v_A}{\sqrt{2}} & \frac{c_{2,2} v_A}{\sqrt{2}} & \frac{c_{2,3} v_A}{\sqrt{2}} & -\frac{c_1 v_d}{\sqrt{2}} & 0 & 0 \\ -\frac{g_1 v_d}{2} & \frac{g_2 v_d}{2} & -\frac{c_1 v_A}{\sqrt{2}} & 0 & 0 & 0 & 0 & -\frac{c_1 v_u}{\sqrt{2}} & 0 & 0 \\ 0 & 0 & \frac{c_{2,1} v_A}{\sqrt{2}} & 0 & 0 & 0 & 0 & \frac{c_{2,1} v_u}{\sqrt{2}} & 0 & 0 \\ 0 & 0 & \frac{c_{2,2} v_A}{\sqrt{2}} & 0 & 0 & 0 & 0 & \frac{c_{2,2} v_u}{\sqrt{2}} & 0 & 0 \\ 0 & 0 & \frac{c_{2,3} v_A}{\sqrt{2}} & 0 & 0 & 0 & 0 & \frac{c_{2,3} v_u}{\sqrt{2}} & 0 & 0 \\ 0 & 0 & -\frac{c_1 v_d}{\sqrt{2}} & -\frac{c_1 v_u}{\sqrt{2}} & \frac{c_{2,1} v_u}{\sqrt{2}} & \frac{c_{2,2} v_u}{\sqrt{2}} & \frac{c_{2,3} v_u}{\sqrt{2}} & 0 & \frac{v_\chi \lambda_\chi}{\sqrt{2}} & \frac{v_{\bar{A}} \lambda_\chi}{\sqrt{2}} \\ 0 & 0 & 0 & 0 & 0 & 0 & 0 & \frac{v_\chi \lambda_\chi}{\sqrt{2}} & 0 & \frac{v_A \lambda_\chi}{\sqrt{2}} \\ 0 & 0 & 0 & 0 & 0 & 0 & 0 & \frac{v_{\bar{A}} \lambda_\chi}{\sqrt{2}} & \frac{v_A \lambda_\chi}{\sqrt{2}} & 0 \end{bmatrix}. \tag{2.14}$$

$\mathcal{M}_{\chi^0}$ was obtained by first implementing our model with the computer program SARAH [53–55], and then setting the sneutrino VEVs to zero, which corresponds to choosing a specific basis [56,57]. This is possible, since the superfields $\hat{H}_d$ and $\hat{L}_i$ have the same quantum numbers in RpV models. The choice of basis is scale dependent, in the sense that sneutrino VEVs are generated by renormalization group (RG) running, even if set to zero at a given scale. Hence, one needs to specify at what scale the basis is chosen. For later convenience, when we compute the axino decays, we choose this scale to be the axino mass. Neglecting for a moment the axino sector, which couples very weakly to the rest, and Takagi diagonalizing the upper-left 7×7 block [58], one finds [20,59] two massless neutrinos and a massive one with

$$m_\nu \approx m_Z \cos^2\beta \sin^2\xi \approx m_Z \cos^2\beta \frac{\kappa_{\rm eff}^2}{\mu_{\rm eff}^2}, \tag{2.15}$$

where

$$\tan\beta = \frac{v_u}{v_d} \quad \text{and} \quad \cos\xi = \frac{\mu_{\rm eff}}{\sqrt{\mu_{\rm eff}^2 + \kappa_{\rm eff,1}^2 + \kappa_{\rm eff,2}^2 + \kappa_{\rm eff,3}^2}}. \tag{2.16}$$

Requiring $m_\nu \approx 0.1$ eV, with $\tan\beta \approx 1$ and $\mu_{\rm eff} \approx 1$ TeV, one finds that $\kappa_{\rm eff,i}$ is of order MeV and correspondingly smaller for larger $\tan\beta$. The two neutrinos which are massless at tree level acquire a small mass at one loop [19,23,24], which we have not included in the 10×10 mass matrix above.

In addition to the neutrinos, there are four eigenstates, mainly built from the MSSM neutralinos ($\lambda_{\tilde{B}}, \tilde{W}^0, \tilde{H}_u^0, \tilde{H}_d^0$), with masses between 100 and 1000 GeV, and three axino eigenstates with masses that can be calculated analytically

in the limit $v_A = v_{\bar{A}} = \frac{f_a}{\sqrt{2}}$, corresponding to $\tan\beta' = 1$, and $c_{1,2} \to 0$. One finds for the axinos [48]

$$-\frac{1}{\sqrt{2}} \lambda_\chi v_\chi, \qquad \frac{1}{2\sqrt{2}} (\lambda_\chi v_\chi \pm \lambda_\chi \sqrt{v_\chi^2 + 4 f_a^2}). \tag{2.17}$$

The lightest of these three states corresponds to the fermionic component of the linear combination of superfields $\frac{1}{\sqrt{2}} (\bar{A} - A)$. It is interpreted as the axino with a mass [48][4]

$$m_{\tilde{a}} \simeq -\frac{1}{\sqrt{2}} \lambda_\chi v_\chi. \tag{2.18}$$

For the more general case of $\tan\beta' \neq 1$, we cannot give analytical expressions. Instead, we find at the lowest order in v_χ / f_a

$$m_{\tilde{a}} \simeq -\frac{\sqrt{2}\tan^2\beta'}{1 + \tan^4\beta'} \lambda_\chi v_\chi + \mathcal{O}\left(\lambda_\chi v_\chi \frac{v_\chi^2}{f_a^2}\right). \tag{2.19}$$

We also give the power of the next term in the expansion, where f_a enters. This is the main contribution to the axino mass, and we neglect small corrections proportional to c_1 and c_2. We expect v_χ to be at the soft SUSY breaking scale, $\mathcal{O}(\text{TeV})$. The Yukawa coupling λ_χ then is our main parameter to control $m_{\tilde{a}}$. λ_χ is radiatively stable: if we set it small at tree level, it remains small. See also Ref. [60] for a quantitative treatment of Yukawa renormalization group equations in supersymmetric models. The most interesting case we consider later is that of a light axino, with $m_{\tilde{a}} = \mathcal{O}(\text{keV})$, which means λ_χ must be very small.

---

[4]Negative fermionic masses can be eliminated by a chiral rotation.

In order to determine the interactions of the axino, in particular the potential decay modes, we would like to estimate the mixing between the axino and the neutrinos. To do this one first diagonalizes the upper 7×7 block, neglecting the axinos which are very weakly coupled. The massive neutrino eigenstate will be mostly a combination of the gauge eigenstates $\nu_{L,i}$, with small components of bino, wino, and Higgsinos. Next include the lower 3×3 axino block. The off-diagonal entries between the neutrino and axino blocks are $c_2 v_u / \sqrt{2} \simeq \kappa_{\text{eff}} v_u / f_a$. Now rotate the 3×3 axino block to the mass eigenstates. The axino is a linear combination of A and $\bar{A}$, and the other two heavier fermions are a combination of A, $\bar{A}$, and χ. The important point is that the entries in the 3×3 Takagi diagonalization axino matrix are of order one. This implies that the pieces in the off-diagonal blocks remain of order $\kappa_{\text{eff}} v_u / f_a$ after rotating the axino block, and we obtain the form of the matrix

$$\mathcal{M}_{\tilde{a},\nu} = \begin{bmatrix} m_\nu & \mathcal{O}\left(\frac{\kappa_{\text{eff}} v}{f_a}\right) \\ \mathcal{O}\left(\frac{\kappa_{\text{eff}} v}{f_a}\right) & m_{\tilde{a}} \end{bmatrix}. \tag{2.20}$$

From this we can read off the axino-neutrino mixing

$$x_{\tilde{a},\nu} \approx \frac{\kappa_{\text{eff}} v}{m_{\tilde{a}} f_a}. \tag{2.21}$$

For the purpose of this estimate and those in Sec. IV, we take $v \equiv \sqrt{v_u^2 + v_d^2} \sim v_u \sim v_d$ to be the weak scale.

The axino-Higgsino mixing can be estimated by observing that the Higgsino mass is of order μ_{eff}, and the off-diagonal element between axino and Higgsino is of order $c_1 v = \frac{\mu_{\text{eff}}}{f_a} v$. Thus, the mixing is

$$x_{\tilde{a},\tilde{H}} \approx \frac{c_1 v}{\mu_{\text{eff}}} = \frac{v}{f_a}. \tag{2.22}$$

Considering $M_1 \sim \mu_{\text{eff}} \sim M_{\text{SUSY}} = \mathcal{O}(\text{TeV})$, we can estimate the bino-Higgsino mixing as $g_1 \frac{v}{M_{\text{SUSY}}}$. Multiplying this times $x_{\tilde{a},\tilde{H}}$ we obtain the axino-bino mixing

$$x_{\tilde{a},\tilde{B}} \approx g_1 \frac{v^2}{M_{\text{SUSY}} f_a}. \tag{2.23}$$

The Higgsino-wino mixing is enhanced by $\cot \theta_W$, with θ_W the Weinberg angle, compared to Higgsino-bino. Hence we write the axino-wino mixing as

$$x_{\tilde{a},\tilde{W}} = \cot \theta_W x_{\tilde{a},\tilde{B}}. \tag{2.24}$$

Next we briefly consider the scalar sector. It is instructive to start by considering the limit $c_{1,2} \to 0$, in which there is no mixing between the MSSM sector and the axion sector, and the axion block of the scalar squared mass matrix can

easily be diagonalized. We find a massless axion and a saxion with a mass squared $\sim m_A^2$ or $m_{\bar{A}}^2$, the parameters in the soft Lagrangian [m_A, $m_{\bar{A}} = \mathcal{O}(\text{TeV})$; cf. Eq. (2.10)]. They are, respectively, the CP-odd and the CP-even mass eigenstates, corresponding to the combination $\frac{1}{\sqrt{2}}(\bar{A} - A)$. The result is not appreciably altered once we turn on the small couplings c_1 and c_2. The other four real scalar degrees of freedom in this sector are heavy, with masses of order $\lambda_\chi f_a$. The masses of the scalars in the MSSM sector are to a very good approximation those already well studied in the RpV SUSY literature [19,60].

III. LIGHT AXINO DECAY MODES

In this section we consider an axino mass lower than twice the electron mass, in which case the axino has only three decay modes:

  (1) into a neutrino and an axion (via a dimension-five operator), $\tilde{a} \to \nu_i + a$;
  (2) into three neutrinos (tree-level), $\tilde{a} \to \nu_i + \nu_j + \nu_k$;
  (3) into a neutrino and a photon (one-loop), $\tilde{a} \to \nu_i + \gamma$.
We discuss them in turn.

A. Decay into neutrino and axion

The dominant operator responsible for the decay $\tilde{a} \to a + \nu$ is dimension five:

$$\frac{1}{f_a} (\partial^\mu a) \bar{\psi}_{\tilde{a}} \gamma_\mu \gamma_5 \psi_{\tilde{a}}. \tag{3.1}$$

This is in the basis of the mass matrix in Eq. (2.20), before we diagonalize to the final mass eigenstate. Here a is the axion, $\psi_{\tilde{a}}$ is the four-component spinor denoting the axino mass eigenstate, and the neutrino arises due to mixing with the axino, once we diagonalize. A simple way to understand the origin of this operator is to consider the kinetic term $\bar{\psi}_{\tilde{a}} \gamma_\mu \partial^\mu \psi_{\tilde{a}}$. After the chiral rotation $\psi_{\tilde{a}} \to e^{i\gamma_5 a/f_a} \psi_{\tilde{a}}$, we obtain the above operator when we expand the exponential. The diagram for the decay is shown in Fig. 1(a), where we include the axino-neutrino mixing [see Eq. (2.21)] in the final state. The partial decay width into this channel is

$$\Gamma_{\tilde{a} \to \nu a} = \frac{x_{\tilde{a},\nu}^2}{16\pi} \frac{m_{\tilde{a}}^3}{f_a^2} \approx \frac{1}{16\pi} \frac{v_u^2 \kappa_{\text{eff}}^2}{f_a^4} m_{\tilde{a}} \tag{3.2}$$

$$= 6 \times 10^{-54} \text{ GeV} \left(\frac{\kappa_{\text{eff}}}{\text{MeV}}\right)^2 \left(\frac{10^{11} \text{ GeV}}{f_a}\right)^4 \left(\frac{m_{\tilde{a}}}{\text{keV}}\right). \tag{3.3}$$

B. Decay into three neutrinos

This tree-level decay proceeds via the axino mixing with the neutrino and the exchange of a Z boson between the fermionic currents, as shown in Fig. 1(b). Assuming for
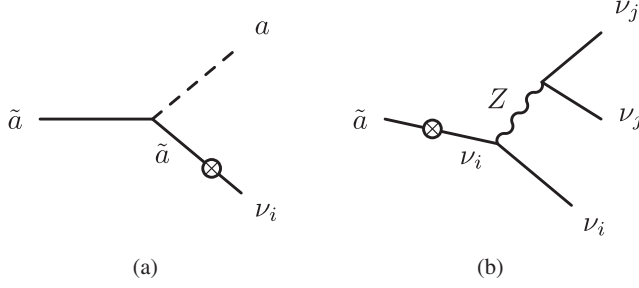
FIG. 1. *Left*: Feynman diagram for the axino decay into an axion and a neutrino, as described by the five-dimensional operator of Eq. (3.1). *Right*: One of the Feynman diagrams describing the decay of the axino into three neutrinos. In our convention the $\otimes$ on a fermion line stands for a mixing between fermionic eigenstates.

simplicity that the neutrino admixture of the axino is measured by $x_{\tilde{a},\nu}$ for *all* neutrino flavors, the decay width into all possible flavors of final neutrinos reads [61]

$$\Gamma_{\tilde{a}\to 3\nu} = \frac{1}{3\pi^3} \frac{G_F^2}{128} x_{\tilde{a},\nu}^2 m_{\tilde{a}}^5 \qquad (3.4)$$

$$= 3 \times 10^{-56} \, \text{GeV} \left(\frac{\kappa_{\text{eff}}}{\text{MeV}}\right)^2 \left(\frac{10^{11} \, \text{GeV}}{f_a}\right)^2 \left(\frac{m_{\tilde{a}}}{\text{keV}}\right)^3. \qquad (3.5)$$

$\Gamma_{\tilde{a}\to 3\nu}$ and $\Gamma_{\tilde{a}\to\nu a}$ give the main contribution to the total decay width in most of the parameter space. We find that for $10^{10} \, \text{GeV} < f_a < 10^{12} \, \text{GeV}$ and $1 \, \text{keV} < m_{\tilde{a}} < 100 \, \text{keV}$, the axino lifetime ranges from 10^{23} to 10^{41} s, which is longer than the age of the universe ($\sim 4 \times 10^{17}$ s).

C. Decay into photon plus neutrino

The one-loop diagrams for the decay $\tilde{a}(p) \to \nu(k_1) + \gamma(k_2)$ have an amplitude with the following structure [62] dictated by gauge invariance:

$$\mathcal{M} = ig_{\tilde{a}\nu\gamma}\bar{u}(k_1)(P_R - \eta_\nu\eta_{\tilde{a}}P_L)\sigma^{\mu\nu}k_{2\mu}\epsilon_\nu^*u(p). \qquad (3.6)$$

Here η_ν and $\eta_{\tilde{a}}$ are the signs of the mass eigenvalues of the neutrino and the axino, respectively, k_2 is the photon momentum, and ϵ is its polarization vector. $g_{\tilde{a}\nu\gamma}$ is a function with the details of the loop integrals and has the dimension of inverse mass. The decay rate then has the form

$$\Gamma_{\tilde{a}\to\nu\gamma} = \frac{|g_{\tilde{a}\nu\gamma}|^2 m_{\tilde{a}}^3}{16\pi}. \qquad (3.7)$$

We are neglecting the final state neutrino mass. The corresponding Feynman diagrams are shown in Figs. 2 and 3. Here we are interested in an estimate, and thus we wish to determine which diagram(s) is (are) dominant. Thus we first consider the individual amplitudes squared, in turn,

as well as the corresponding decay width, without including interference terms. If not otherwise specified, we make use of the formulas provided in Ref. [63] to compute the loop integrals. We do not include diagrams with sneutrino VEV insertions (see e.g., Ref. [64]), since, as previously mentioned, we work in the basis, defined at the axino mass scale, where such VEVs are zero.

The first diagrams we consider are those depicted in Figs. 2(a) and 2(b). The corresponding decay width has been computed in the analogous case of a sterile neutrino decaying into a neutrino and a photon [65] (see also Ref. [66] for a review),

$$\Gamma_{\nu(Wl)} = \frac{9\alpha G_F^2}{1024\pi^4} x_{\tilde{a},\nu}^2 m_{\tilde{a}}^5 \approx \frac{9\alpha G_F^2}{1024\pi^4} \frac{\kappa_{\text{eff}}^2 v_u^2}{f_a^2} m_{\tilde{a}}^3$$

$$= 3 \times 10^{-58} \, \text{GeV} \left(\frac{\kappa_{\text{eff}}}{\text{MeV}}\right)^2 \left(\frac{10^{11} \, \text{GeV}}{f_a}\right)^2 \left(\frac{m_{\tilde{a}}}{\text{keV}}\right)^3. \qquad (3.8)$$

Here, the first subscript on Γ indicates the state the incoming axino mixes with, while the subscripts in parentheses denote the particles running in the loop. We use this notation for the rest of the section. Let us anticipate that in most of the parameter space we consider, $\Gamma_{\nu(Wl)}$ gives the dominant contribution. It is therefore useful to compare the other partial widths to $\Gamma_{\nu(Wl)}$. Incidentally, a decay width of $\Gamma_{\tilde{a}} = 3 \times 10^{-58}$ GeV corresponds to a lifetime $\tau_{\tilde{a}} = 2 \times 10^{23}$ s and the lifetime of the universe is about $\tau_{\text{univ}} \approx 4 \times 10^{17}$ s.

The main contribution to the two diagrams in Figs. 2(c) and 2(d) comes from the heaviest lepton that can run in the loop, the τ. We have

$$\Gamma_{(Hl)} \approx \frac{m_{\tilde{a}}^3}{2^{11}\pi^5} \frac{\kappa_{\text{eff}}^2}{f_a^2} \left(\frac{B\mu}{m_{H^\pm}^2}\right)^2 Y_\tau^2 \frac{m_\tau^2}{m_{H^\pm}^4} \ln^2\left(\frac{m_\tau^2}{m_{H^\pm}^2}\right). \qquad (3.9)$$

The m_τ^2 in the numerator comes from the mass insertion that flips the chirality in the fermion line in the loop, while $B\mu/m_{H^\pm}^2$ is an estimate of the mixing between the charged scalar Higgses, $B\mu$ being the bilinear parameter in the Higgs potential; see Eq. (2.10). Taking $B\mu \sim m_{H^\pm}^2$ as an estimate, we find the ratio

$$\frac{\Gamma_{(Hl)}}{\Gamma_{\nu(Wl)}} = \frac{1}{18\pi\alpha G_F^2} \frac{Y_\tau^2}{v_u^2} \frac{m_\tau^2}{m_{H^\pm}^4} \ln^2\left(\frac{m_\tau^2}{m_{H^\pm}^2}\right)$$

$$\approx 3 \times 10^{-8} \left(\frac{m_{H^\pm}}{\text{TeV}}\right)^{-4} \frac{\ln^2\left(\frac{m_\tau^2}{m_{H^\pm}^2}\right)}{160}, \qquad (3.10)$$

which is highly suppressed, and we neglect the contributions from the corresponding diagrams in the following.

Next we consider the diagrams of Figs. 2(e) and 2(f). We assume the $\tilde{\tau}$ to be the lightest charged slepton and give the leading contribution. We find
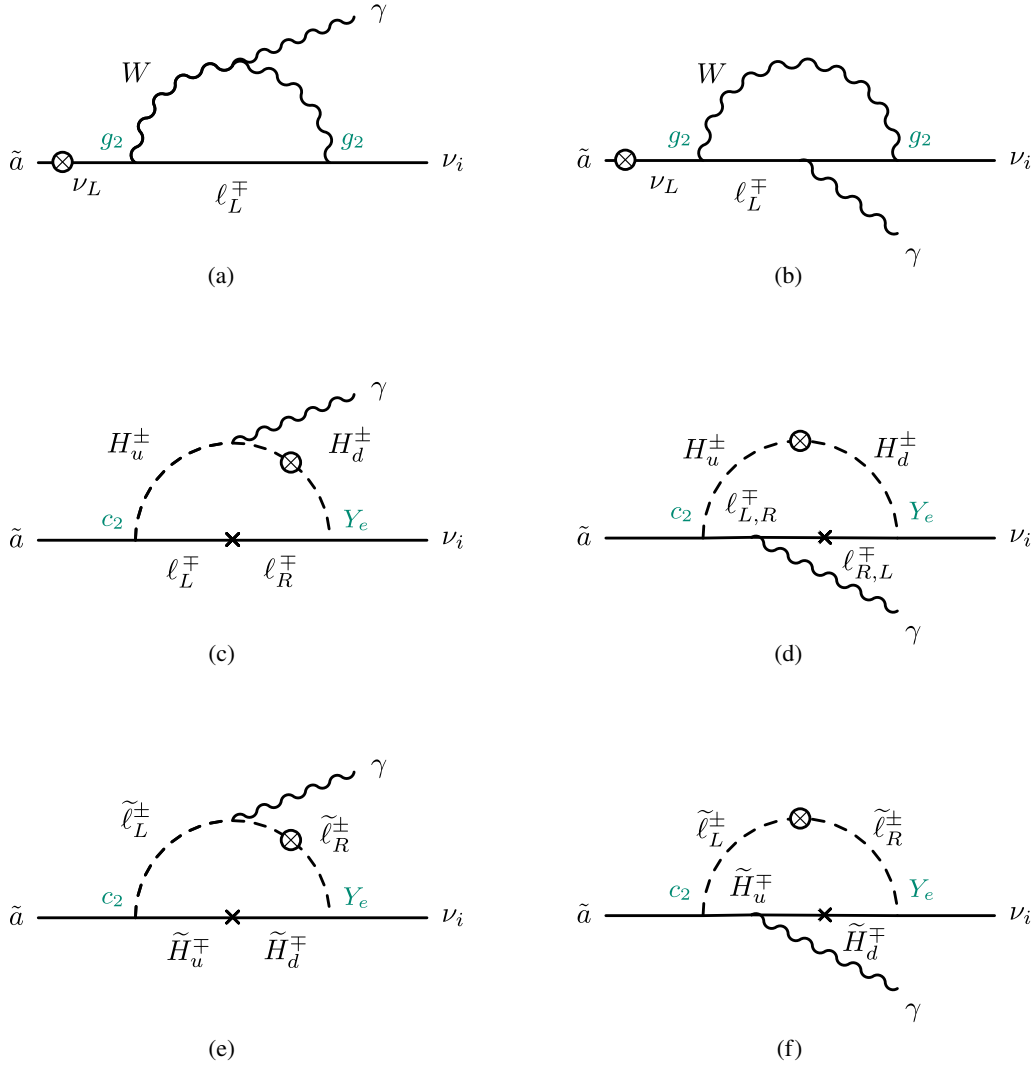
FIG. 2. Diagrams with no dependence on the RpV trilinear couplings $\lambda^{(\prime)}$. The cross on a fermion line indicates a mass insertion needed for the chirality flip, while the $\otimes$ on a scalar or fermion line is a (dimensionless) mixing. We write the coupling constants in green at the vertices.

$$\Gamma_{(\tilde{H}\tilde{l})} \approx \frac{m_{\tilde{a}}^3}{2^{11}\pi^5} \frac{\kappa_{\text{eff}}^2}{f_a^2} x_{\tilde{\tau}_{LR}}^2 Y_{\tilde{\tau}}^2 \frac{\mu_{\text{eff}}^2}{m_{\tilde{\tau}}^4} \frac{\left(1 + \ln\frac{\mu_{\text{eff}}^2}{m_{\tilde{\tau}}^2} - \frac{\mu_{\text{eff}}^2}{m_{\tilde{\tau}}^2}\right)^2}{\left(1 - \frac{\mu_{\text{eff}}^2}{m_{\tilde{\tau}}^2}\right)^4}. \quad (3.11)$$

Here, $x_{\tilde{\tau}_{LR}} \approx \frac{\mu_{\text{eff}} m_\tau}{m_{\tilde{\tau}}^2} \tan\beta$ is the mixing between the left and right staus, and μ_{eff} is the Higgsino mass. Note that the expression is finite in the limit $\mu_{\text{eff}} = m_{\tilde{\tau}}$. We find the ratio

$$\frac{\Gamma_{(\tilde{H}\tilde{l})}}{\Gamma_{\nu(Wl)}} = \frac{1}{18\pi\alpha G_F^2} \frac{Y_{\tilde{\tau}}^2}{v_u^2} \frac{\mu_{\text{eff}}^4 m_\tau^2}{m_{\tilde{\tau}}^8} \tan^2\beta \frac{\left(1 + \ln\frac{\mu_{\text{eff}}^2}{m_{\tilde{\tau}}^2} - \frac{\mu_{\text{eff}}^2}{m_{\tilde{\tau}}^2}\right)^2}{\left(1 - \frac{\mu_{\text{eff}}^2}{m_{\tilde{\tau}}^2}\right)^4}$$

$$\approx 10^{-12} \tan^2\beta \left(\frac{\mu_{\text{eff}}}{\text{TeV}}\right)^4 \left(\frac{m_{\tilde{\tau}}}{2 \text{ TeV}}\right)^{-8}. \quad (3.12)$$

This is also highly suppressed, and we neglect it in the following.

Next, we examine the diagrams of Fig. 3, which involve at least one trilinear RpV coupling, λ or λ'. To avoid

cluttering the equations, we use λ to denote either. For the diagrams of Figs. 3(a) and 3(b) we find

$$\Gamma_{\tilde{B}(f\tilde{f})} \approx N_c^2 \frac{m_{\tilde{a}}^3 Q_f^2}{2^{11}\pi^5} g_1^2 \lambda^2 x_{\tilde{a},\tilde{B}}^2 \frac{m_f^2}{m_{\tilde{f}}^4} \ln^2\left(\frac{m_f^2}{m_{\tilde{f}}^2}\right), \quad (3.13)$$

and for the diagrams of Figs. 3(c) and 3(d)

$$\Gamma_{\tilde{W}(f\tilde{f})} \approx N_c^2 \frac{m_{\tilde{a}}^3 Q_f^2}{2^{11}\pi^5} g_2^2 \lambda^2 x_{\tilde{a},\tilde{w}}^2 \frac{m_f^2}{m_{\tilde{f}}^4} \ln^2\left(\frac{m_f^2}{m_{\tilde{f}}^2}\right). \quad (3.14)$$

The latter is a factor of $\cot^4\theta_W = (g_2/g_1)^4 = 12.57$ larger than the former,

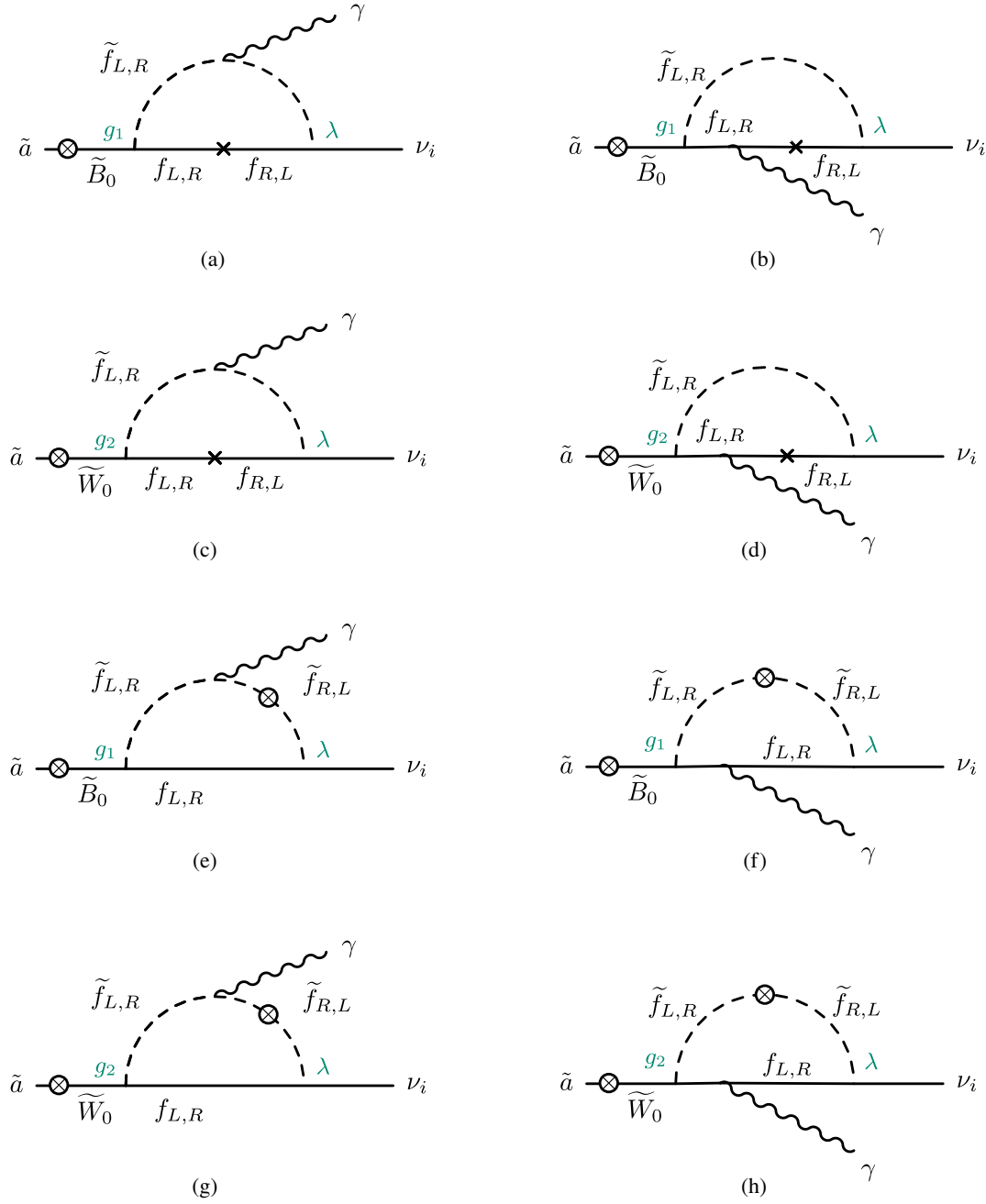$$\Gamma_{\tilde{W}(f\tilde{f})} = \cot^4\theta_W \Gamma_{\tilde{B}(f\tilde{f})}. \quad (3.15)$$

FIG. 3. Diagrams with an explicit dependence on the RpV trilinear couplings $\lambda^{(\prime)}$ where the axino mixes with the bino or the wino. The notation is the same as in Fig. 2.

In these formulas, N_C is the number of colors of the fermions/sfermions running in the loop. f ($\tilde{f}$) denotes either a down-type quark (squark), in the case of a λ' coupling, or a lepton (slepton), in the case of a λ coupling. Q_f is the electric charge of f in units of e, $g_1 = e/\cos\theta_W$ the hypercharge gauge coupling, $g_2 = e/\cos\theta_W$ the $SU(2)_L$ gauge coupling, $x_{\tilde{a},\tilde{B}}$ the axino-bino mixing from Eq. (2.23), and $x_{\tilde{a},\tilde{W}}$ the axino-wino mixing from Eq. (2.24). The largest contribution to Eq. (3.13) and Eq. (3.14) comes from a loop of bottom-sbottom. Comparing $\Gamma_{\bar{W}(f\tilde{f})}$ to Eq. (3.8), we find

$$\frac{\Gamma_{\bar{W}(f\tilde{f})}}{\Gamma_{\nu(Wl)}} = \frac{N_c^2 g_2^4 Q_f^2}{18\pi\alpha G_F^2} \frac{\lambda^2 v^2}{M_{\text{SUSY}}^2 \kappa_{\text{eff}}^2} \frac{m_f^2}{m_{\tilde{f}}^4} \ln^2\left(\frac{m_{\tilde{f}}^2}{m_{\tilde{f}}^2}\right)$$

$$\approx 20 \left(\frac{N_c}{3}\right)^2 \left(\frac{\lambda}{10^{-2}}\right)^2 \left(\frac{Q_f}{1/3}\right)^2 \left(\frac{\text{MeV}}{\kappa_{\text{eff}}}\right)^2$$

$$\times \left(\frac{\text{TeV}}{M_{\text{SUSY}}}\right)^2 \left(\frac{m_f}{m_b}\right)^2 \left(\frac{\text{TeV}}{m_{\tilde{f}}}\right)^4 \frac{\ln^2\left(\frac{m_{\tilde{f}}^2}{m_{\tilde{f}}^2}\right)}{120}, \quad (3.16)$$

where m_b is the mass of the bottom quark. We see that $\Gamma_{\bar{W}(f\tilde{f})}$, even considering $m_{\tilde{f}} > 1$ TeV as motivated by recent
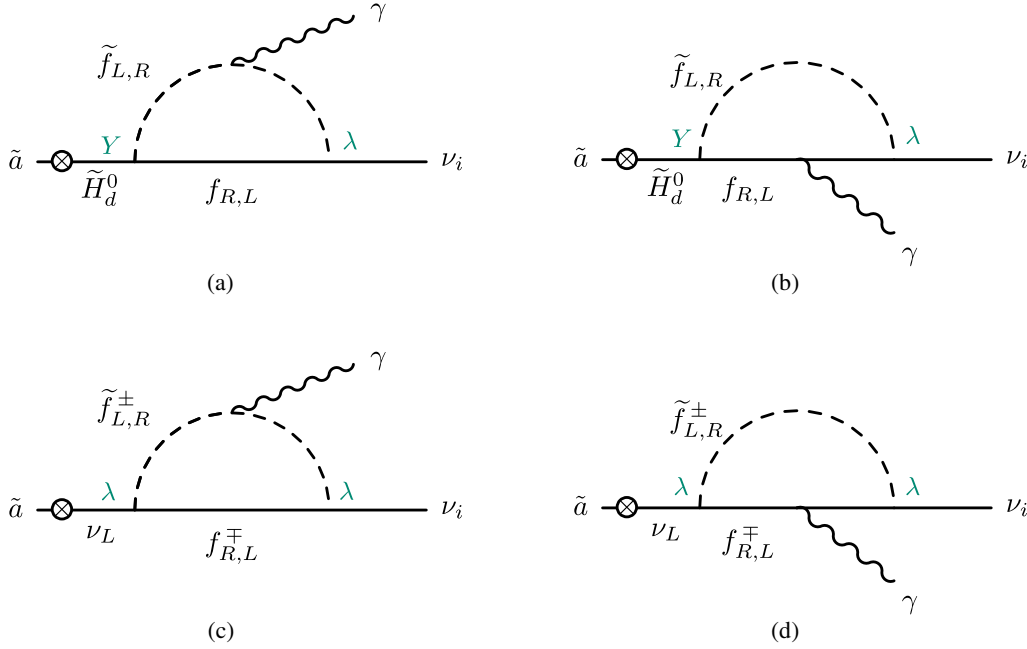
FIG. 4. Diagrams with an explicit dependence on the RpV trilinear couplings $\lambda^{(\prime)}$ where the axino mixes with the Higgsino or the neutrino.

analyses [6,67] which disfavor lighter squarks and sleptons, can give a contribution larger than $\Gamma_{\nu(Wl)}$. We comment further on this contribution below. Diagrams in Figs. 3(e), 3(f), 3(g), and 3(h) differ from those of Figs. 3(a), 3(b), 3(c), and 3(d) in that there is no mass insertion in the propagator of the fermion, but there is a mixing in the sfermion line in the loop. Again the contribution from diagrams where the axino mixes with the wino is larger. We estimate the decay width corresponding to Figs. 3(g) and 3(h) to be

$$\tilde{\Gamma}_{\tilde{W}(f\tilde{f})} \approx N_c^2 \frac{m_{\tilde{a}}^3 Q_f^2}{2^{11}\pi^5} g_2^2 \lambda^2 x_{\tilde{a},\tilde{W}}^2 x_{\tilde{f}_{LR}}^2 \frac{m_{\tilde{a}}^2}{m_{\tilde{f}}^4} \ln^2\left(\frac{m_f^2}{m_{\tilde{f}}^2}\right), \quad (3.17)$$

where $x_{\tilde{f}_{LR}} \approx \frac{\mu_{\text{eff}} m_f}{m_{\tilde{f}}^2} \tan\beta$ is the mixing between left and right sfermions. We have

$$\frac{\tilde{\Gamma}_{\tilde{W}(f\tilde{f})}}{\Gamma_{\tilde{W}(f\tilde{f})}} \approx \frac{m_{\tilde{a}}^2}{m_{\tilde{f}}^2} \frac{\mu_{\text{eff}}^2}{m_{\tilde{f}}^2} \tan^2\beta \ll 1, \quad (3.18)$$

due to $m_{\tilde{a}} \ll m_{\tilde{f}}$, and the same suppression for $\tilde{\Gamma}_{\tilde{B}(f\tilde{f})}$. As a result, both $\tilde{\Gamma}_{\tilde{W}(f\tilde{f})}$ and $\tilde{\Gamma}_{\tilde{B}(f\tilde{f})}$ are negligible compared to $\Gamma_{\tilde{W}(f\tilde{f})}$ and $\Gamma_{\tilde{B}(f\tilde{f})}$.

For the diagrams of Figs. 4(a) and 4(b) we find (note there is no mass insertion in the fermion line in the loop)

$$\Gamma_{\tilde{H}(f\tilde{f})} \approx N_c^2 \frac{m_{\tilde{a}}^3 Q_f^2}{2^{11}\pi^5} Y^2 \lambda^2 x_{\tilde{a},\tilde{H}}^2 \frac{m_{\tilde{a}}^2}{m_{\tilde{f}}^4} \ln^2\left(\frac{m_f^2}{m_{\tilde{f}}^2}\right). \quad (3.19)$$

Here, $f(\tilde{f})$ can be either a down-type quark (squark), in the case of a λ' coupling, or a lepton (slepton), in the case of a λ coupling. Y is either the Y_d or the Y_e Yukawa, and the axino-Higgsino mixing is given in Eq. (2.22). As in the previous case, the main contribution to these diagrams is
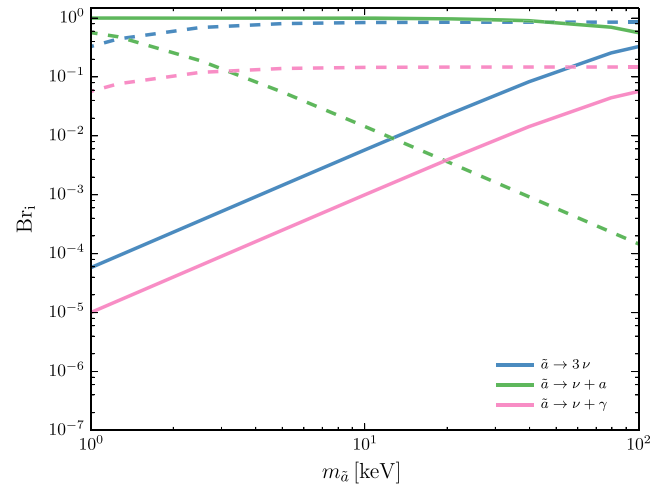

FIG. 5. We show the branching ratios of the axino decay channels into axion and neutrino, three neutrinos, photon and neutrino, as a function of the axino mass. The total width is $\Gamma_{\tilde{a}\to a\nu} + \Gamma_{\tilde{a}\to 3\nu} + \Gamma_{\tilde{a}\to\gamma\nu}$, where in $\Gamma_{\tilde{a}\to\gamma\nu}$ we take into account only the three dominant contributions, $\Gamma_{\tilde{W}(f\tilde{f})} + \Gamma_{\tilde{B}(f\tilde{f})} + \Gamma_{\nu(Wl)}$, as discussed in the main text. We consider a loop of bottom-sbottom for the evaluation of $\Gamma_{\tilde{W}(f\tilde{f})}$ and $\Gamma_{\tilde{B}(f\tilde{f})}$, with $m_{\tilde{b}} = 1$ TeV, and an RpV trilinear coupling $\lambda = 10^{-2}$. Continuous (dashed) lines are for $f_a = 10^{10}$ GeV ($f_a = 10^{12}$ GeV).

TABLE II. Upper bounds on the magnitude of R-parity violating couplings at the 2σ confidence level, taken from Ref. [6]. The constraints arise from indirect decays. The concrete processes are described in detail in Ref. [68].

ijk	$\lambda_{ijk}(M_W)$	$\lambda'_{ijk}(M_W)$
133	$0.0060 \times \sqrt{\frac{m_{\tilde{\tau}}}{100\ \mathrm{GeV}}}$	$0.0014 \times \sqrt{\frac{m_{\tilde{b}}}{100\ \mathrm{GeV}}}$
233	$0.070 \times \frac{m_{\tilde{\tau}_R}}{100\ \mathrm{GeV}}$	$0.15 \times \sqrt{\frac{m_{\tilde{b}}}{100\ \mathrm{GeV}}}$
333	$\cdots$	$0.45\ (1.04)$

from the bottom-sbottom loop. $\Gamma_{\tilde{H}(f\tilde{f})}$ is suppressed compared to $\Gamma_{\tilde{B}(f\tilde{f})}$ by a factor of $m_{\tilde{a}}^2/m_{\tilde{f}}^2$. We have

$$\frac{\Gamma_{\tilde{H}(f\tilde{f})}}{\Gamma_{\nu(Wl)}} = \frac{N_c^2 Q_f^2}{18\pi\alpha G_F^2} \frac{\lambda^2 Y^2}{\kappa_{\mathrm{eff}}^2} \frac{m_{\tilde{a}}^2}{m_{\tilde{f}}^4} \ln^2\left(\frac{m_f^2}{m_{\tilde{f}}^2}\right)$$

$$\approx 10^{-11} \left(\frac{N_c}{3}\right)^2 \left(\frac{\lambda}{10^{-2}}\right)^2 \left(\frac{Q_f}{1/3}\right)^2 \left(\frac{Y}{Y_b}\right)^2$$

$$\times \left(\frac{\mathrm{MeV}}{\kappa_{\mathrm{eff}}}\right)^2 \left(\frac{m_{\tilde{a}}}{10\ \mathrm{keV}}\right)^2 \left(\frac{\mathrm{TeV}}{m_{\tilde{f}}}\right)^4 \frac{\ln^2\left(\frac{m_f^2}{m_{\tilde{f}}^2}\right)}{120}.$$

$$(3.20)$$

The last two diagrams to evaluate are those of Figs. 4(c) and 4(d). The two RpV couplings appearing in each of these diagrams have no restrictions on their flavor index structure, contrary to those of Figs. 3(a) to 4(b), which are diagonal in the singlet-doublet mixings. For the sake of our discussion we also do not distinguish between the two potentially different λ here, as we consider only one RpV coupling to be different from zero at a time. We find

$$\Gamma_{\nu(f\tilde{f})} \approx N_c^2 \frac{m_{\tilde{a}}^3 Q_f^2}{2^{11}\pi^5} \lambda^4 x_{\tilde{a},\nu}^2 \frac{m_{\tilde{a}}^2}{m_{\tilde{f}}^4} \ln^2\left(\frac{m_f^2}{m_{\tilde{f}}^2}\right), \qquad (3.21)$$
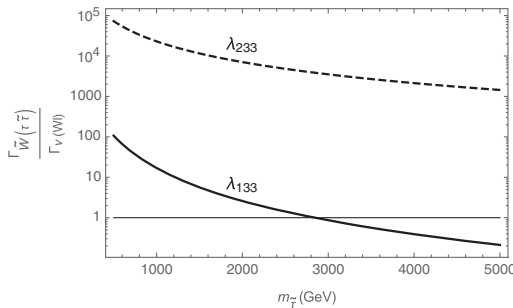
the main contributions being again from bottom-sbottom and tau-stau loops, and

$$\frac{\Gamma_{\nu(f\tilde{f})}}{\Gamma_{\nu(Wl)}} = \frac{N_c^2 Q_f^2}{18\pi\alpha G_F^2} \frac{\lambda^4}{m_{\tilde{f}}^4} \left(\log\frac{m_f^2}{m_{\tilde{f}}^2}\right)^2$$

$$\approx 10^{-8} \left(\frac{N_c}{3}\right)^2 \left(\frac{\lambda}{10^{-2}}\right)^4 \left(\frac{Q_f}{1/3}\right)^2$$

$$\times \left(\frac{\mathrm{TeV}}{m_{\tilde{f}}}\right)^4 \frac{\ln^2\left(\frac{m_f^2}{m_{\tilde{f}}^2}\right)}{120}. \qquad (3.22)$$

From our estimates we see that $\Gamma_{\tilde{W}(f\tilde{f})}, \Gamma_{\tilde{B}(f\tilde{f})}$, and $\Gamma_{\nu(Wl)}$ give the dominant contributions, the other diagrams being always negligible. Thus the axion decay width into photon and neutrino is given to a good approximation by $\Gamma_{\tilde{W}(f\tilde{f})} + \Gamma_{\tilde{B}(f\tilde{f})} + \Gamma_{\nu(Wl)}$. In Fig. 5 we plot the branching ratios corresponding to the three decay channels of our light axino.

It is worth examining $\Gamma_{\tilde{W}(f\tilde{f})}$ in more detail. First, we reintroduce the generation indices in the superpotential terms

$$\frac{1}{2}\lambda_{ijk}\hat{L}_i\hat{L}_j\hat{\bar{E}}_k + \lambda'_{ijk}\hat{L}_i\hat{Q}_j\hat{\bar{D}}_k. \qquad (3.23)$$

As the main contributions to $\Gamma_{\tilde{W}(f\tilde{f})}$ are from tau-stau and bottom-sbottom loops, the trilinear couplings of interest are those shown in Table II. The first index of λ_{ijk} and λ'_{ijk} refers, in our case, to the neutrino in the lepton doublet. We see in Fig. 6 that when we consider the decay $\tilde{a} \to \nu_2\gamma$, with λ_{233} and λ'_{233} saturating the upper bounds in Table II, the diagrams giving $\Gamma_{\tilde{W}(f\tilde{f})}$ provide the dominant contribution.

We can use this fact to set new bounds on these trilinear couplings by considering constraints from x rays and gamma rays [69,70] on the decays $\tilde{a} \to \nu_{2,3}\gamma$. We proceed as follows. First, we assume that the entire dark matter is
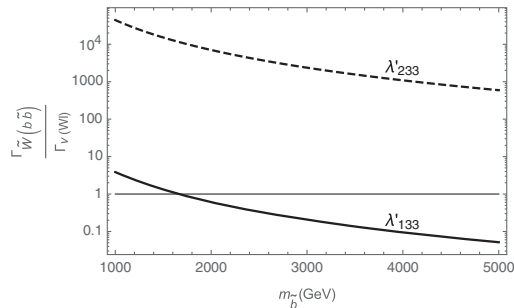

FIG. 6. We show the ratio $\frac{\Gamma_{\tilde{W}(f\tilde{f})}}{\Gamma_{\nu(Wl)}}$ from Eq. (3.16) as a function of the sfermion mass. We have set $M_{\mathrm{SUSY}} = 1$ TeV and $\kappa_{\mathrm{eff}} = 1$ MeV. The left plot corresponds to the tau-stau loop, with $m_f = m_\tau$. The solid line is obtained by taking $\lambda = \lambda_{133} = 0.006\sqrt{\frac{m_{\tilde{\tau}}}{100\ \mathrm{GeV}}}$, while for the dashed line $\lambda = \lambda_{233} = 0.07\frac{m_{\tilde{\tau}}}{100\ \mathrm{GeV}}$. The right plot corresponds to the bottom-sbottom loop, with $m_f = m_b$. The solid line is obtained by taking $\lambda' = \lambda'_{133} = 0.0014\sqrt{\frac{m_{\tilde{b}}}{100\ \mathrm{GeV}}}$, while for the dashed line $\lambda = \lambda'_{233} = 0.15\sqrt{\frac{m_{\tilde{b}}}{100\ \mathrm{GeV}}}$. The values chosen for the trilinear couplings saturate the up-to-date bounds of Table II.
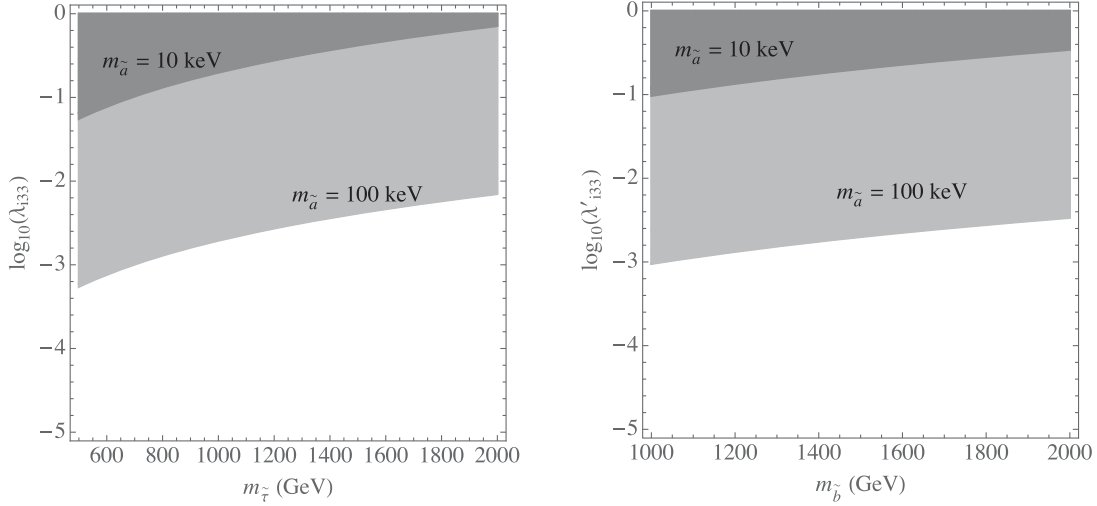
FIG. 7. We show regions excluded by x- and gamma-ray constraints [69,70]. Here we use Eq. (3.24) and assume the axino to contribute to the totality of dark matter. The dark (light) gray region is excluded when $m_{\tilde{a}} = 10$ keV (100 keV). In λ'_{i33}, the index i can be either 2 or 3, in which case the dominant contribution to the decay $\tilde{a} \to \nu_i \gamma$ is from $\Gamma_{\tilde{W}(f\tilde{f})}$.

constituted by the axino, $\Omega_{\tilde{a}} h^2 = \Omega_{\mathrm{DM}}$. This fixes f_a for any given value of $m_{\tilde{a}}$. Then the excluded region corresponds to

$$\Gamma_{\tilde{W}(f\tilde{f})} > \Gamma_{\mathrm{bound}} = \frac{1}{\tau_{\mathrm{bound}}}, \qquad (3.24)$$

where τ_{bound} is given, for instance, in Fig. 9 of Ref. [70] as a function of the mass of the decaying particle, the axino in our case. In Fig. 7 we see that, for $m_{\tilde{a}} = 100$ keV, we can set bounds on the trilinears $\lambda_{233}, \lambda'_{233}, \lambda'_{333}$ of order 10^{-3}. These are to be compared with the bounds in Table II. However, it is important to keep in mind that these new bounds, contrary to those in Table II, rely on the presence of the axino and on the assumption that it is the whole dark matter.

In Fig. 10 we show the x- and gamma-ray constraints on the plane f_a vs m_a. The excluded regions in purple correspond to

$$\frac{\Omega_{\tilde{a}}}{\Omega_{\mathrm{DM}}} \Gamma_{\tilde{a} \to \nu\gamma} > \Gamma_{\mathrm{bound}} = \frac{1}{\tau_{\mathrm{bound}}}. \qquad (3.25)$$

Here, $\Gamma_{\tilde{a} \to \nu\gamma} = \max[\Gamma_{\tilde{W}(f\tilde{f})}, \Gamma_{\nu(Wl)}]$, and we multiply by $\Omega_{\tilde{a}}/\Omega_{\mathrm{DM}}$ to account for the region of parameter space where the axino is underabundant. We discuss the axino relic abundance in Sec. IV.

D. Comment on the 3.5 keV line

This model can fit the 3.5 keV line observed in galaxy clusters [40–42,44]. A possible benchmark point, for instance, is the following:

$$m_{\tilde{a}} = 7 \text{ keV}, \quad f_a = 3.5 \times 10^{10} \text{ GeV},$$
$$m_{\tilde{b}} = 2 \text{ TeV}, \quad \lambda'_{233} = 0.07. \qquad (3.26)$$

With these values, the axino constitutes the entire dark matter and has a partial decay width $\Gamma_{\tilde{a} \to \nu\gamma} \approx \Gamma_{\tilde{W}(f\tilde{f})} \approx 6 \times 10^{-53}$ GeV, needed to explain the putative line. The benchmark complies with the bounds we mentioned above. We emphasize, however, that evidence that the 3.5 keV line is due to decaying DM is not conclusive [71–79].

IV. COSMOLOGICAL AND ASTROPHYSICAL CONSTRAINTS

A. The gravitino

We assume a supergravity completion of our model, with SUSY broken at a high scale ($\sqrt{F} \sim 3 \times 10^{10}$ GeV) and the breaking effects mediated via Planck suppressed operators, so that the soft scale is $M_{\mathrm{SUSY}} \sim \frac{F}{M_{\mathrm{Pl}}} = \mathcal{O}(\mathrm{TeV})$. The gravitino is heavy, with $m_{3/2} \sim M_{\mathrm{SUSY}}$, decays before big bang nucleosynthesis, and poses no cosmological problems.

B. The saxion

In the context of supersymmetric axion models one usually has to worry about the saxion: if it is too light, it can pose serious issues (see e.g., Ref. [80]). We briefly review why. The saxion is a pseudomodulus, meaning that its potential is quite flat. During inflation we expect it to sit at a distance of order f_a from the minimum of its zero-temperature potential. After inflation, when the Hubble parameter H becomes comparable to the saxion mass, m_s, the saxion starts to oscillate about its minimum. From the condition $H(T_s^{\mathrm{osc}}) \sim m_s$, with $H(T) \sim \frac{T^2}{M_{\mathrm{Pl}}}$, we find the temperature at which the oscillations start,

$$T_s^{\mathrm{osc}} \sim \sqrt{m_s M_{\mathrm{Pl}}}. \qquad (4.1)$$

At that time the energy density in the oscillating field is $\rho_s \sim m_s^2 f_a^2$. The energy density of radiation is $\rho_r \sim (T_s^{\mathrm{osc}})^4$, so that $\left(\frac{\rho_s}{\rho_r}\right)_{\mathrm{osc}} \sim \frac{f_a^2}{M_{\mathrm{Pl}}^2}$. The energy density of the oscillating saxion scales as T^3, behaving like matter, which implies that in the absence of decays it would come to dominate the energy density of the universe at a temperature

$$T_s^{\mathrm{dom}} \sim \frac{f_a^2}{M_{\mathrm{Pl}}^2} T_s^{\mathrm{osc}} \sim \frac{f_a^2}{M_{\mathrm{Pl}}^2} \sqrt{m_s M_{\mathrm{Pl}}}. \tag{4.2}$$

It is important to determine whether it decays before or after domination. To proceed with this simple estimate we parametrize the decay rate as $\Gamma_s \sim \frac{1}{16\pi} \frac{m_s^3}{f_a^2}$, neglecting the masses of the decay products. The factor of f_a^2 at the denominator is due to the fact that the saxion couplings to matter are suppressed by f_a. Then the decay temperature is obtained from $H(T_s^{\mathrm{dec}}) \sim \Gamma_s$:

$$T_s^{\mathrm{dec}} \sim \frac{m_s^{3/2} M_{\mathrm{Pl}}^{1/2}}{10 f_a}. \tag{4.3}$$

From these estimates we find

$$\frac{T_s^{\mathrm{dec}}}{T_s^{\mathrm{dom}}} \sim 10^4 \left(\frac{m_s}{1 \text{ TeV}}\right)\left(\frac{10^{12} \text{ GeV}}{f_a}\right)^3. \tag{4.4}$$

In our model the saxion mass is of order TeV, so it decays way before it comes to dominate the energy density of the universe.[5] Note the temperature when it decays is of order GeV, safely above big bang nucleosynthesis.

C. Axion dark matter

In this model the axion is a dark matter candidate. We do not review here the calculations of its relic abundance, but refer the reader to Refs. [83,84]. There are two possible mechanisms to produce axion cold DM, which depend on whether the PQ symmetry is spontaneously broken before or after the end of inflation. In the former case, axion DM is solely produced via the misalignment mechanism, which results in the abundance

$$\Omega_{a,\mathrm{mis}}h^2 = 0.18\theta_1^2 \left(\frac{f_a}{10^{12} \text{ GeV}}\right)^{1.19}\left(\frac{\Lambda_{\mathrm{QCD}}}{400 \text{ MeV}}\right). \tag{4.5}$$

Here θ_1 is the initial misalignment angle. If the PQ symmetry is broken after the end of inflation, on top of this contribution there is another one coming from non-relativistic axions emitted by global strings:

---

[5]A saxion that comes to dominate the energy density can have other interesting implications; see e.g., Refs. [81,82].

$$\Omega_{a,\mathrm{str}}h^2 \approx 0.2\xi\bar{r}\left(\frac{f_a}{10^{12} \text{ GeV}}\right)^{1.19}\left(\frac{\Lambda_{\mathrm{QCD}}}{400 \text{ MeV}}\right). \tag{4.6}$$

These strings are topological field configurations containing loops in space where the axion field wraps the domain $[0, 2\pi f_a]$ nontrivially [85,86]. In Eq. (4.6), ξ is the length parameter which represents the average number of strings in a horizon volume. It is determined by numerical simulations [87], $\xi \simeq 1.0$. The parameter $\bar{r}$ is related to the average energy of the axions emitted in string decays. Its value has been the subject of a long debate. Two scenarios have been put forth: one predicts $\bar{r} \approx 1$, and the other $\bar{r} \approx 70$. See Ref. [85] and references therein for details and Ref. [86] for recent considerations on the issue.

While the misalignment mechanism produces axions when the temperature is $T \sim \Lambda_{\mathrm{QCD}}$, the strings form at a much higher temperature $T \sim f_a$. If the PQ phase transition happened before the end of inflation, or equivalently if the reheating temperature (T_{RH}) were lower than f_a, then the strings would be inflated away and we would no longer have a contribution corresponding to Eq. (4.6). In this scenario the axion abundance is from Eq. (4.5), and θ_1 can take any value between $-\pi$ and π. In the scenario with the PQ phase transition post inflation ($T_{\mathrm{RH}} > f_a$), one has to average θ_1^2 over many QCD horizons, $\langle\theta_1^2\rangle = \pi^2/3$, and the contribution from string decays can be comparable to that from misalignment or larger, depending on the value of $\bar{r}$.

D. A heavy axino

For $\lambda_\chi \sim 1$, we have $m_{\tilde{a}} \sim v_\chi \sim M_{\mathrm{SUSY}}$, an axino mass of order TeV. Such an axino has many open decay channels into MSSM particles, with a total width that can be estimated as $\Gamma_{\tilde{a}} \sim \frac{1}{8\pi} \frac{m_{\tilde{a}}^3}{f_a^2}$. It decays safely before big bang nucleosynthesis and does not pose cosmological issues.

E. A light axino

The axino, if light, can also be a dark matter candidate [39,88–93]. It was pointed out in Ref. [39] that for $T_{\mathrm{RH}} > f_a$ a stable axino should not exceed the mass of 1 or 2 keV; otherwise, it would result in overabundant DM. More recently Bae *et al.* [84,94] showed that the axino production rate is suppressed if $M_\Phi \ll f_a$, where M_Φ is the mass of the heaviest PQ-charged and gauge-charged matter supermultiplet in the model. This suppression is significant in DFSZ models, where M_Φ corresponds to the Higgsino mass. The consequence of such a suppression is that the upper bound of 2 keV on the axino mass quoted in Ref. [39] is relaxed. In our model the axino is not stable. However, if its mass is below the electron mass, the only decay modes are the following:

(1) into a neutrino and an axion (tree-level, with dimension-five operator), $\tilde{a} \to \nu_i + a$;
(2) into three neutrinos (tree-level), $\tilde{a} \to \nu_i + \nu_j + \nu_k$;
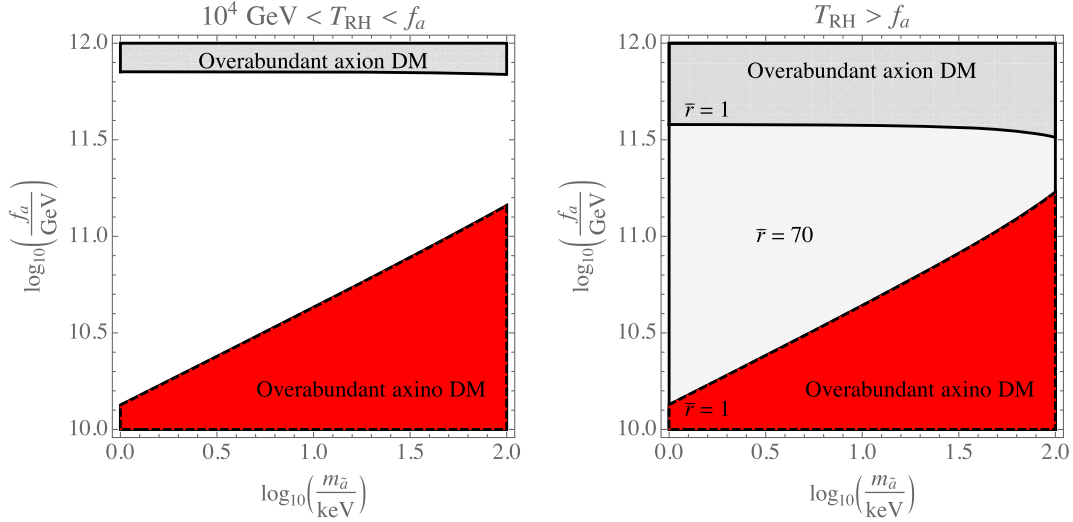(3) into a neutrino and a photon (one-loop), $\tilde{a} \to \nu_i + \gamma$.

FIG. 8.   We show, in the plane f_a vs the axino mass $m_{\tilde{a}}$, the regions where the combination of axion and the axino dark matter exceeds the observed abundance, $(\Omega_a + \Omega_{\tilde{a}})h^2 > \Omega_{\text{DM}}h^2 = 0.12$ [96]. In the grey region the main contribution is from the axion, and in the red from the axino [Eq. (4.7)]. Along the black solid line the axion alone results in the correct abundance, while along the black dashed line the axino alone accounts for Ω_{DM}. In the left panel the reheat temperature, T_{RH}, is below the PQ phase transition scale, f_a, and the only contribution to axion dark matter is from the misalignment mechanism, Eq. (4.5). Here we take the initial misalignment angle $\theta_1 = 1$. In the white region, the combination of axion plus axino results in a total abundance below Ω_{DM}. In the right panel T_{RH} is above f_a, and we also have a contribution to axion dark matter from the decay of axionic strings, Eq. (4.6). We show the excluded region for two different values of the parameter $\bar{r}$. Note that for $\bar{r} = 70$, the axion plus axino are overabundant on the entire plane. Furthermore, the lifetime of the axino is longer than the age of the universe in the entire region plotted.

The resulting lifetime, as we showed in Sec. III, is longer than the age of the universe, thus making the axino a dark matter candidate, with relic abundance (see Sec. 3.1 and Appendix C in Ref. [84] for a derivation of this result)

$$\Omega_{\tilde{a}}h^2 \simeq 2.1 \times 10^{-5} \left(\frac{m_{\tilde{a}}}{1 \text{ keV}} \right) \left(\frac{10^{12} \text{ GeV}}{f_a} \right)^2. \quad (4.7)$$

This does not depend on T_{RH}, as long as $T_{\text{RH}} > 10^4$ GeV [84,94]. For lower T_{RH} and different cosmological histories

the axion abundance can be different [95], but we will not consider such scenarios in this work. We learn that, for $f_a = 10^{12}$ GeV, the axino can have a mass as large as a few MeV before it becomes overabundant. The important feature of Eq. (4.7) is that the abundance is inversely proportional to f_a^2. It is easy to understand why. The axino never reaches thermal equilibrium in the early universe because its interactions are very weak. It is produced in scattering processes (listed e.g., in Table 1 of Ref. [84]) with a cross section
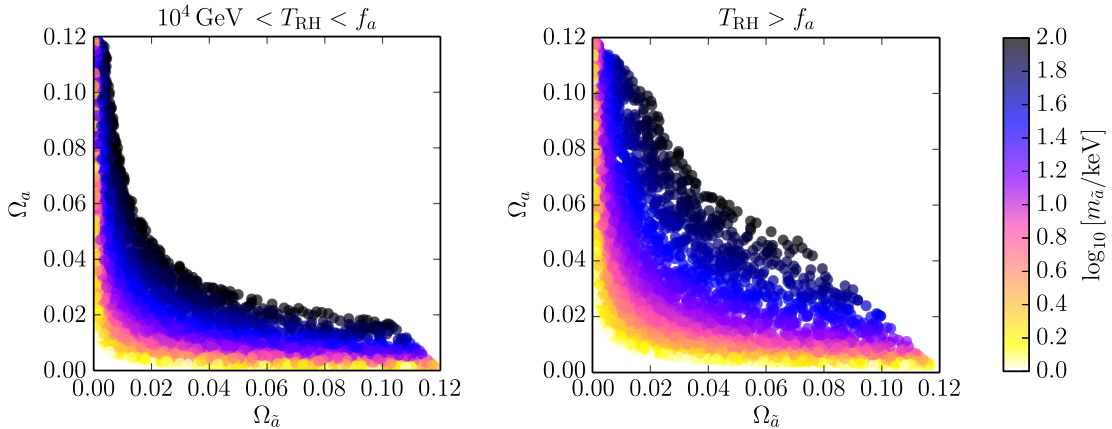

FIG. 9.   Scatter plot of the allowed parameter space in the plane $\Omega_a h^2$ against $\Omega_{\tilde{a}} h^2$. In the left panel ($T_{\text{RH}} < f_a$) we have only the misalignment contribution to the axion relic density, with $\theta_1 = 1$, while in the right panel ($T_{\text{RH}} > f_a$) we also have the contribution from decays of axionic strings, for which we fix $\bar{r} = 1$. At each point f_a is selected randomly within the range $[10^{10}, 10^{12}]$ GeV, in both plots. The value of $m_{\tilde{a}}$, shown in the color bar, is then obtained by using Eq. (4.7). We only show points for which the sum of axion and axino abundances is within the observed dark matter abundance, $\Omega_{\text{DM}}h^2 = 0.12$.
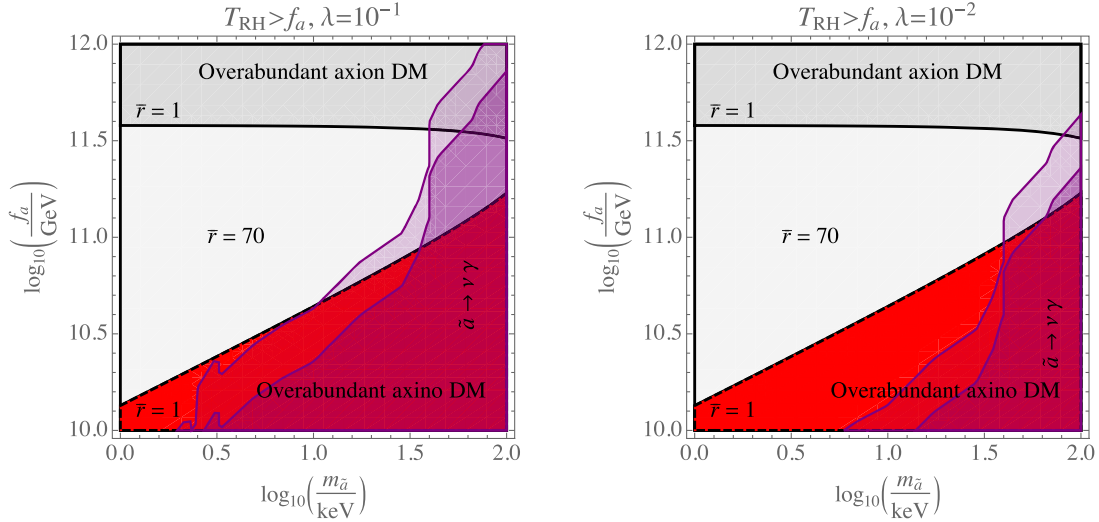
FIG. 10. We add to the right plot of Fig. 8 the constraints from x rays and gamma rays [see Eq. (3.25)], shown in light purple. When these regions overlap with the red region, the parameter space is excluded by the overabundance of the axino. On the left we set the trilinear coupling to $\lambda = 10^{-1}$, and on the right $\lambda = 10^{-2}$. The lighter (darker) purple region corresponds to a mass of the sfermion, running in the loop, of 1 (2) TeV.

proportional to $1/f_a^2$. The larger the cross section the more the axino is produced, hence the $1/f_a^2$ dependence in Eq. (4.7). In Fig. 8 we show the allowed region of parameter space, in the plane f_a vs $m_{\tilde{a}}$, for axion and axino dark matter. In Fig. 9 we show scatter plots in the plane $\Omega_a h^2$ vs $\Omega_{\tilde{a}} h^2$. It is apparent from this figure that when $T_{\mathrm{RH}} < f_a$, so that the only contribution to the axion relic is from misalignment, the dark matter relic is dominated by either one of the two species. On the other hand, for $T_{\mathrm{RH}} > f_a$, when we have also the contribution from string decays, there are regions of parameter space in which axions and axinos contribute almost equally to the total relic. In Fig. 10 we add the constraints from x rays and gamma rays, discussed in the previous section.

V. SUMMARY

We have presented for the first time a complete RpV SUSY model with baryon triality and with a DFSZ axion superfield. We have studied the mass spectrum and then investigated some cosmological bounds. The axion is a good dark matter candidate when its decay constant $f_a = \mathcal{O}(10^{11})$ GeV. For lower values of f_a the axino, with a mass roughly between 1 and 100 keV, can be the dominant dark matter candidate. We have looked at the possible decay modes of the light axino in detail. For such a light axino, its lifetime is longer than the age of the universe, but its decay into photon and neutrino still leads to interesting phenomenology. We have shown that x- and gamma-ray constraints on this decay give new bounds on some trilinear RpV couplings. These are model dependent and rely on the axino constituting the whole dark matter in the universe. We have also shown that in this model there is

a corner of parameter space where a 7 keV axino could fit the 3.5 keV line observed in galaxy clusters.

This model, like any axion model (whether supersymmetric or not), is very difficult to test at colliders. The main reason is that the coupling to the Higgs portal, c_1 in our specific case, must be very small for the axion to be invisible [33]. As a consequence, both the axion and the axino couple very weakly to the rest of the MSSM and elude a possible detection at colliders. If SUSY were eventually discovered and turned out to be R-parity violating, this model would provide two compelling dark matter candidates in that context. At present the best experimental tests of this scenario are in astrophysics and cosmology, which were the focus of the current work. If we discovered warm dark matter in the keV mass range, together with a striking signature from x rays, this model would represent a possible explanation. In such a case the experimental evidence would not be enough to distinguish this scenario from that of a sterile neutrino, for example. More evidence from other observables, ideally in laboratories or at colliders, would be necessary, but as we said that is difficult to achieve. Our model also has a connection between axino and neutrino physics, which is very suppressed as well due to the smallness of the coupling c_2, dictated by the bound on neutrino masses. Perhaps in the far future new and more precise data in neutrino physics will provide another possible experimental test.

APPENDIX A: THE UNBEARABLE LIGHTNESS OF THE AXION

The axino mass has been extensively discussed in the literature [39,97–100]. It is commonly held to be highly model dependent, taking on almost any value [89,92]. In this Appendix we point out that a keV mass axino is more easily embedded in the DFSZ class of models rather than in the KSVZ models [46,47]. We then discuss how the mass is related to the PQ and SUSY breaking energy scales.

1. KSVZ vs DFSZ

Axion models fall into two broad categories denoted as KSVZ and DFSZ. Both contain a complex scalar field, $A(x)$, charged under a global $U(1)_{PQ}$, PQ symmetry [49]. The axion field, $a(x)$, is identified with the phase of $A(x)$.[6] In the KSVZ model, $A(x)$ couples to exotic heavy quark fields, $Q(x)$, that are charged under color and under the $U(1)_{PQ}$ [and possibly $U(1)_{EM}$], while the rest of the SM fields do not carry any PQ charge. The coupling $f_Q A \bar{Q} Q$ generates, via a triangle diagram, the interaction term $a G_{\mu\nu} \tilde{G}^{\mu\nu}$ which is crucial in solving the strong CP problem. Here $G_{\mu\nu}(x)$ is the gluon field strength tensor and $\tilde{G}^{\mu\nu}(x)$ its dual. In the supersymmetric version, the KSVZ model is defined by the superpotential $W_{KSVZ} = f_Q \hat{A} \hat{\bar{Q}} \hat{Q}$, where we use hats to denote chiral superfields and Q and $\bar{Q}$ are two distinct superfields in the **3** and **3̄** representations of $SU(3)_c$, respectively, but with equal PQ charge. Embedding the model in supergravity results in a one-loop contribution to the axino mass of order [39,101]

$$m_{\tilde{a}} \sim 10 \text{ GeV} \left(\frac{m_{3/2} f_Q^2}{100 \text{ GeV}} \right), \tag{A1}$$

where $m_{3/2}$ is the gravitino mass. Moreover, even if supergravity effects are neglected, there is an irreducible two-loop contribution involving the gluino [102]

$$m_{\tilde{a}} \sim 0.3 \text{ GeV} \left(\frac{m_{\tilde{g}} f_Q^2}{1 \text{ TeV}} \right), \tag{A2}$$

where $m_{\tilde{g}}$ is the gluino mass. This implies that even if the axino mass is tuned to keV values at tree level, loop

---

[6]This is not rigorously exact in the DFSZ models, but true to a good approximation.

corrections tend to raise it to GeV values. Thus a KSVZ axino prefers to be heavier than a few keV.

In DFSZ models the field $A(x)$ couples to two Higgs doublets, H_u and H_d, which are also charged under the $U(1)_{PQ}$, as well as the other SM fields are. Thus the supersymmetric version of the DFSZ axion model is more economical than the KSVZ counterpart, as SUSY already requires at least two Higgs doublets. The SUSY coupling of axions to Higgses can be written as [39] $W_{DFSZ} = c_1 \hat{A} \hat{H}_u \hat{H}_d$. The field A has to get a large VEV $\langle A \rangle \sim f_a$, with $f_a > 10^9$ GeV; otherwise, the corresponding axion would be excluded by supernova constraints [50]. In turn, this implies a tiny coupling c_1. Note that the corresponding coupling in nonsupersymmetric DFSZ models also has to be very small for the axion to be invisible. In the SUSY context it has been proposed that the operator $c_1 \hat{A} \hat{H}_u \hat{H}_d$ could be replaced [103] by a nonrenormalizable one $\frac{g}{M_{Pl}} \hat{A}^2 \hat{H}_u \hat{H}_d$. With the latter operator one easily obtains a μ-term at the TeV scale, while with the former we are forced to take very small values for the coupling c_1. We do not address the μ-problem, but we point out that Ref. [104] showed that the operator we consider can be derived consistently within a string theory framework. The fact that c_1 is tiny helps with the axino mass: once we set it to keV values at tree level we are guaranteed that radiative corrections, proportional to c_1, will be negligible as opposed to the KSVZ case we discussed above.

2. Low-scale vs high-scale SUSY breaking

In a previous paper [48], we indicated a simple way to understand that in models where the SUSY breaking scale, M_{SB}, is lower than the PQ scale, f_a, the axino mass is of order $\mathcal{O}(\frac{M_{SUSY}^2}{f_a})$, with M_{SUSY} the scale of the soft supersymmetry breaking terms, while in models with $M_{SB} > f_a$ the axino mass is typically of order M_{SUSY}. The former models, with low M_{SB}, are representative of global SUSY, for which the best known framework is gauge mediation of supersymmetry breaking [105]. The latter ones, with high M_{SB}, usually fall in the scheme of gravity mediation of supersymmetry breaking [106–108], in local supersymmetry, and the scale of the soft terms is that of the gravitino mass, $M_{SUSY} \sim m_{3/2}$.

In light of these considerations one would think that a light axino is more natural in the context of gauge mediation. However, it turns out that this is difficult to accommodate. The problem is with the saxion. Consider a model of minimal gauge mediation (see e.g., Ref. [105]), where the messengers do not carry any PQ charge and communicate with the visible sector only via gauge interactions. The leading contribution to the mass of the sfermions of the MSSM is generated at two loops. However, the saxion is a gauge singlet, and its mass can be generated only at three loops, as shown schematically in Fig. 11. The coupling c_1 that appears twice in the diagram
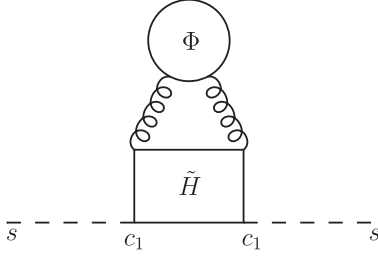
FIG. 11.   Three-loop contribution to the saxion mass in minimal gauge mediation. At the top we have a loop of messenger fields, Φ, drawn as a circle, and at the bottom a loop of Higgsinos, drawn as a rectangle. The wiggly lines are gauge bosons. The coupling c_1 of the saxion to the Higgsinos is defined in Eq. (2.3).

is the one we discussed in the previous subsection, and the same that appears in the superpotential of Eq. (2.1). The saxion squared mass, m_s^2, is suppressed by a factor of $\sim \frac{c_1^2}{16\pi^2}$ compared to the squared masses of the MSSM sfermions, $m_{\tilde{f}}^2$, so we can estimate

$$m_s \sim 0.1 \text{ keV} \left(\frac{c_1}{10^{-9}}\right) \left(\frac{m_{\tilde{f}}}{1 \text{ TeV}}\right). \qquad (A3)$$

This light saxion could pose serious cosmological problems [109] as it would come to dominate the energy density of the universe for a long time before it decays. We reviewed some of the issues associated with saxion cosmology in Sec. IV. One way out of this problem would be to make the saxion heavier. This could be achieved by coupling the axion superfield either to the messengers or to fields in the hidden sector responsible for SUSY breaking. Apart from the extra field content that the procedure would bring into the model there is another issue that seems difficult to overcome: the same couplings needed to make the saxion heavier would very likely produce a heavy axino [110]. Perhaps there is a clever way to arrange for a heavy saxion and a light axino in gauge mediation, but in light of our considerations it seems that such a model would have to be quite complicated. We do not investigate this aspect further in this work. Rather we choose a supergravity (SUGRA) model. We showed in Ref. [48] that in SUGRA the axino would typically have a mass comparable to the gravitino, thus in the TeV range. However, we can adjust a single parameter, λ_χ, to lower the axino mass down to the keV range. Doing so does not affect other masses, such as those of saxion and gravitino for instance. Also, as we argued above, since the axino we consider is of the DFSZ type, once we set its mass at tree level it will not be affected appreciably by loop corrections. Therefore the SUGRA model can be kept minimal, as opposed to a possible model with gauge mediation, at the expense of some tuning, needed to lower the mass of the axino. In the model presented in this paper the axino is much lighter than the

gravitino. This represents an explicit exception to the generic argument that the axino should be heavier than the gravitino, put forward in Ref. [111].

APPENDIX B: AXINO-GAUGINO MIXING

Most of the amplitudes involved in the radiative decay of the axino bear a strong dependence on its mixing with some of the other neutralino mass eigenstates. In this work we rely on well-motivated estimates for these quantities, but in order to obtain their precise values one should diagonalize the neutralino mass matrix $\mathcal{M}_{\chi^0}$. While an exact analytical algorithm exists for the case of the MSSM [112], adding one more mass eigenstate, as for the case of the next-to-minimal supersymmetric Standard Model (NMSSM), does not allow for a closed-form solution. In this section we show how the approximate block-diagonalization procedure of Ref. [113] for the NMSSM 5×5 neutralino mass matrix can be used to obtain a numerical value for the axino-gaugino mixing. The only requirement is a small mixing between the singlet and the doublet states, which in our case corresponds to the mixing between any of the two Higgs doublets and the axion field A. From $\mathcal{M}_{\chi^0}$ in Eq. (2.14) we see that such mixing is indeed small, since $\frac{c_1 v_{u,d}}{\sqrt{2}} \approx \frac{\mu_{\text{eff}}}{f_a} \lesssim 10^{-7}$. Recalling that the axino mass eigenstate consists of a linear combination of the fermionic components of the fields A and $\bar{A}$ only, we define the following neutralino mass 5×5 submatrix:

$$\mathcal{M}_5 = \begin{bmatrix} M_1 & 0 & \frac{g_1 v_u}{2} & -\frac{g_1 v_d}{2} & 0 \\ 0 & M_2 & -\frac{g_2 v_u}{2} & \frac{g_2 v_d}{2} & 0 \\ \frac{g_1 v_u}{2} & -\frac{g_2 v_u}{2} & 0 & -\frac{c_1 v_A}{\sqrt{2}} & -\frac{c_1 v_d}{\sqrt{2}} \\ -\frac{g_1 v_d}{2} & \frac{g_2 v_d}{2} & -\frac{c_1 v_A}{\sqrt{2}} & 0 & -\frac{c_1 v_u}{\sqrt{2}} \\ 0 & 0 & -\frac{c_1 v_d}{\sqrt{2}} & -\frac{c_1 v_u}{\sqrt{2}} & m_{\tilde{a}} \end{bmatrix}, \qquad (B1)$$

where the axino mass $m_{\tilde{a}}$ is the lightest eigenvalue which results from the diagonalization of the 3×3 lower-right block of the neutralino mass matrix $\mathcal{M}_{\chi^0}$ in Eq. (2.14). The diagonalization of $\mathcal{M}_5$ proceeds in two steps: first, the 4×4 matrix V rotates only the MSSM upper-left 4×4 block into a diagonal form; next a second matrix block diagonalizes the full resulting 5×5 matrix, in a way that the 4×4 MSSM submatrix $\mathcal{M}_4$ is still diagonal up to corrections of the second order in the singlet-doublet mixing parameter $\frac{\mu_{\text{eff}}}{f_a}$. The 5×5 unitary matrix U which combines these two steps is

$$U = \begin{bmatrix} \mathbb{1}_4 - \frac{1}{2}(V\Lambda)(V\Lambda)^T & (V\Lambda) \\ -(V\Lambda)^T & 1 - \frac{1}{2}(V\Lambda)^T(V\Lambda) \end{bmatrix} \begin{bmatrix} V & 0 \\ 0 & 1 \end{bmatrix},$$
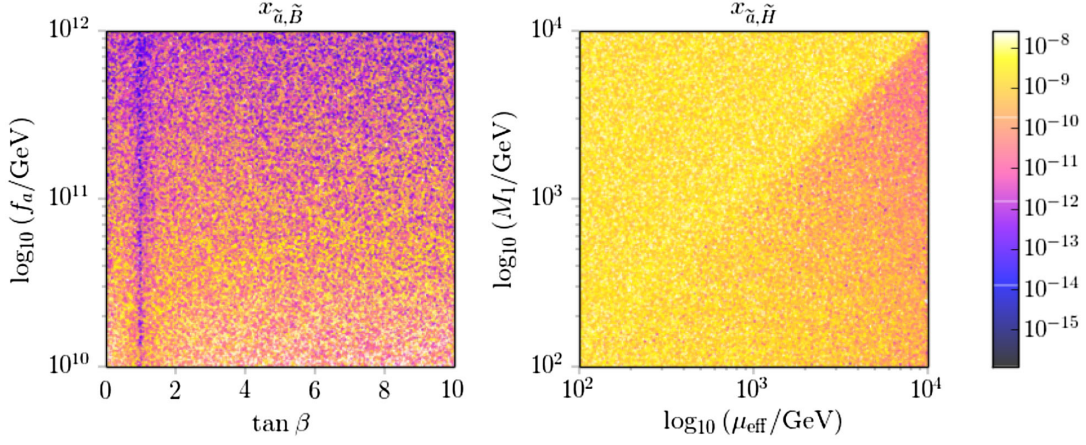
$$(B2)$$

FIG. 12. Distribution of the mixings $x_{\tilde{a},\tilde{B}}$ and $x_{\tilde{a},\tilde{H}}$ obtained by numerical evaluation of the eigenvalues of $\mathcal{M}_4$. We run 10^5 points randomly varying 10^2 GeV $< M_{1,2}$, $\mu_{\text{eff}} < 10^4$ GeV, $1 < \tan\beta < 10$, 10^{10} GeV $< f_a < 10^{12}$ GeV, and 1 keV $< m_{\tilde{a}} < 10^2$ keV. From our estimate in Eq. (2.22) [Eq. (2.23)] we expect $x_{\tilde{a},\tilde{H}}$ [$x_{\tilde{a},\tilde{B}}$] to lie somewhere in the range between approximately 10^{-10} and 10^{-8} GeV [10^{-12} and 10^{-10} GeV], depending on the value of f_a.

with

$$
\Lambda = -\frac{m_{\tilde{a}}}{\det(\mathcal{M}_4 - \mathbb{1}_4 m_{\tilde{a}})}
\begin{bmatrix}
(M_2 - m_{\tilde{a}})g_1 \frac{v}{2}\mu_{\text{eff}}\cos 2\beta \\
(M_1 - m_{\tilde{a}})g_2 \frac{v}{2}\mu_{\text{eff}}\cos 2\beta \\
(M_1 - m_{\tilde{a}})(M_2 - m_{\tilde{a}})(\mu_{\text{eff}}\sin\beta - m_{\tilde{a}}\cos\beta) - M_\star^3 \cos\beta \\
(M_1 - m_{\tilde{a}})(M_2 - m_{\tilde{a}})(\mu_{\text{eff}}\cos\beta - m_{\tilde{a}}\sin\beta) - M_\star^3 \sin\beta
\end{bmatrix}
\tag{B3}
$$

and $M_\star^3 = \frac{v^2}{4}[(M_1 - m_{\tilde{a}})g_2^2 + (M_2 - m_{\tilde{a}})g_1^2]$. The axino-gaugino mixings can then be read off from the off-diagonal entry $\sum_{j=1}^4 V_{ij}\Lambda_j$ of U, with $j = \tilde{B}_0, \tilde{W}_0, \tilde{H}_u^0, \tilde{H}_d^0$. In Fig. 12 we show two examples of how a more careful analysis can change significantly such quantities, and thus ultimately the phenomenology of the model. This possibly constitutes caveats to our above reasoning. In the left panel we observe that a value of $\tan\beta$ close to 1 strongly suppresses the value of $x_{\tilde{a},\tilde{B}}$, such that our previous estimates are off by several orders of magnitude. In the right panel instead we see how allowing for larger values of μ_{eff} might lower $x_{\tilde{a},\tilde{H}}$, if $M_1 < \mu$.

[1] E. Gildener, Gauge symmetry hierarchies, Phys. Rev. D **14**, 1667 (1976).

[2] M. J. G. Veltman, The infrared–ultraviolet connection, Acta Phys. Pol. B **12**, 437 (1981).

[3] G. R. Farrar and P. Fayet, Phenomenology of the production, decay, and detection of new hadronic states associated with supersymmetry, Phys. Lett. **76B**, 575 (1978).

[4] G. L. Kane, C. F. Kolda, L. Roszkowski, and J. D. Wells, Study of constrained minimal supersymmetry, Phys. Rev. D **49**, 6173 (1994).

[5] P. Bechtle et al., How alive is constrained SUSY really?, Nucl. Phys. B, Proc. Suppl. **273–275**, 589 (2016).

[6] D. Dercks, H. K. Dreiner, M. E. Krauss, T. Opferkuch, and A. Reinert, R-parity violation at the LHC, Eur. Phys. J. C **77**, 856 (2017).

[7] E. Aprile et al. (XENON Collaboration), First Dark Matter Search Results from the XENON1T Experiment, Phys. Rev. Lett. **119**, 181301 (2017).

[8] D. S. Akerib et al. (LUX Collaboration), Results from a Search for Dark Matter in the Complete Lux Exposure, Phys. Rev. Lett. **118**, 021303 (2017).

[9] A. Tan et al. (PandaX-II Collaboration), Dark Matter Results from First 98.7 Days of Data from the Pandax-Ii Experiment, Phys. Rev. Lett. **117**, 121303 (2016).

[10] S. Weinberg, Supersymmetry at ordinary energies. 1. Masses and conservation laws, Phys. Rev. D **26**, 287 (1982).

[11] H. K. Dreiner, C. Luhn, and M. Thormeier, What is the discrete gauge symmetry of the Mssm?, Phys. Rev. D **73**, 075007 (2006).

[12] H. K. Dreiner, C. Luhn, H. Murayama, and M. Thormeier, Proton hexality from an anomalous flavor U(1) and neutrino masses: Linking to the string scale, Nucl. Phys. **B795,** 172 (2008).

[13] L. E. Ibanez and G. G. Ross, Discrete gauge symmetry anomalies, Phys. Lett. B **260,** 291 (1991).

[14] S. P. Martin, A supersymmetry primer, Adv. Ser. Dir. High Energy Phys. **18,** 1 (1997).

[15] Y. Grossman and H. E. Haber, (S)Neutrino properties in R-parity violating supersymmetry. 1. CP conserving phenomena, Phys. Rev. D **59,** 093008 (1999).

[16] H. K. Dreiner, C. Luhn, H. Murayama, and M. Thormeier, Baryon triality and neutrino masses from an anomalous flavor U(1), Nucl. Phys. **B774,** 127 (2007).

[17] H. K. Dreiner, J. Soo Kim, and M. Thormeier, A simple baryon trialitymodel for neutrino masses, arXiv:0711.4315.

[18] M. A. Bernhardt, S. P. Das, H. K. Dreiner, and S. Grab, Sneutrino as lightest supersymmetric particle in B_3 Msugra models and signals at the LHC, Phys. Rev. D **79,** 035003 (2009).

[19] B. C. Allanach, A. Dedes, and H. K. Dreiner, R parity violating minimal supergravity model, Phys. Rev. D **69,** 115002 (2004); Erratum, Phys. Rev. D **72,** 079902(E) (2005).

[20] L. J. Hall and M. Suzuki, Explicit R-parity breaking in supersymmetric models, Nucl. Phys. **B231,** 419 (1984).

[21] E. Nardi, Renormalization group induced neutrino masses in supersymmetry without R-parity, Phys. Rev. D **55,** 5772 (1997).

[22] A. Abada and M. Losada, Constraints on a general three generation neutrino mass matrix from neutrino data: Application to the MSSM with R-parity violation, Nucl. Phys. **B585,** 45 (2000).

[23] M. Hirsch, M. A. Diaz, W. Porod, J. C. Romao, and J. W. F. Valle, Neutrino masses and mixings from supersymmetry with bilinear R parity violation: A theory for solar and atmospheric neutrino oscillations, Phys. Rev. D **62,** 113008 (2000); Erratum, Phys. Rev. D **65,** 119901(E) (2002).

[24] S. Davidson and M. Losada, Neutrino masses in the R-parity violating MSSM, J. High Energy Phys. 05 (2000) 021.

[25] A. H. Chamseddine and H. K. Dreiner, Anomaly free gauged R symmetry in local supersymmetry, Nucl. Phys. **B458,** 65 (1996).

[26] H. M. Lee, S. Raby, M. Ratz, G. G. Ross, R. Schieren, K. Schmidt-Hoberg, and P. K. S. Vaudrevange, A unique $\mathbb{Z}_4^R$ symmetry for the MSSM, Phys. Lett. B **694,** 491 (2011).

[27] H. M. Lee, S. Raby, M. Ratz, G. G. Ross, R. Schieren, K. Schmidt-Hoberg, and P. K. S. Vaudrevange, Discrete R symmetries for the MSSM and its singlet extensions, Nucl. Phys. **B850,** 1 (2011).

[28] H. K. Dreiner, T. Opferkuch, and C. Luhn, Froggatt-Nielsen models with a residual $\mathbb{Z}_4^R$ symmetry, Phys. Rev. D **88,** 115005 (2013).

[29] M.-C. Chen, M. Ratz, and V. Takhistov, R parity violation from discrete R symmetries, Nucl. Phys. **B891,** 322 (2015).

[30] R. D. Peccei, The strong CP problem and axions, Lect. Notes Phys. **741,** 3 (2008).

[31] F. Wilczek, Problem of Strong P and T Invariance in the Presence of Instantons, Phys. Rev. Lett. **40,** 279 (1978).

[32] S. Weinberg, A New Light Boson?, Phys. Rev. Lett. **40,** 223 (1978).

[33] M. Dine, W. FischLer, and M. Srednicki, A simple solution to the strong CP problem with a harmless axion, Phys. Lett. **104B,** 199 (1981).

[34] A. R. Zhitnitsky, On possible suppression of the axion hadron interactions, Sov. J. Nucl. Phys. **31,** 260 (1980).

[35] J. Preskill, M. B. Wise, and F. Wilczek, Cosmology of the invisible axion, Phys. Lett. **120B,** 127 (1983).

[36] R. Holman, G. Lazarides, and Q. Shafi, Axions and the dark matter of the Universe, Phys. Rev. D **27,** 995 (1983).

[37] L. F. Abbott and P. Sikivie, A cosmological bound on the invisible axion, Phys. Lett. **120B,** 133 (1983).

[38] M. Dine and W. Fischler, The not so harmless axion, Phys. Lett. **120B,** 137 (1983).

[39] K. Rajagopal, M. S. Turner, and F. Wilczek, Cosmological implications of axinos, Nucl. Phys. **B358,** 447 (1991).

[40] E. Bulbul, M. Markevitch, A. Foster, R. K. Smith, M. Loewenstein, and S. W. Randall, Detection of an unidentified emission line in the stacked X-ray spectrum of galaxy clusters, Astrophys. J. **789,** 13 (2014).

[41] A. Boyarsky, O. Ruchayskiy, D. Iakubovskyi, and J. Franse, Unidentified Line in X-Ray Spectra of the Andromeda Galaxy and Perseus Galaxy Cluster, Phys. Rev. Lett. **113,** 251301 (2014).

[42] J.-C. Park, S. C. Park, and K. Kong, X-ray line signal from 7 keV axino dark matter decay, Phys. Lett. B **733,** 217 (2014).

[43] K.-Y. Choi and O. Seto, X-ray line signal from decaying axino warm dark matter, Phys. Lett. B **735,** 92 (2014).

[44] S. P. Liew, Axino dark matter in light of an anomalous X-ray line, J. Cosmol. Astropart. Phys. 05 (2014) 044.

[45] S. Colucci, H. K. Dreiner, F. Staub, and L. Ubaldi, Heavy concerns about the light axino explanation of the 3.5 keV X-ray line, Phys. Lett. B **750,** 107 (2015).

[46] J. E. Kim, Weak Interaction Singlet and Strong CP Invariance, Phys. Rev. Lett. **43,** 103 (1979).

[47] M. A. Shifman, A. I. Vainshtein, and V. I. Zakharov, Can confinement ensure natural CP invariance of strong interactions?, Nucl. Phys. **B166,** 493 (1980).

[48] H. K. Dreiner, F. Staub, and L. Ubaldi, From the unification scale to the weak scale: A self consistent supersymmetric Dine-Fischler-Srednicki-Zhitnitsky axion model, Phys. Rev. D **90,** 055016 (2014).

[49] R. D. Peccei and H. R. Quinn, CP Conservation in the Presence of Instantons, Phys. Rev. Lett. **38,** 1440 (1977).

[50] G. G. Raffelt, Astrophysical axion bounds, Lect. Notes Phys. **741,** 51 (2008).

[51] F. D'Eramo, L. J. Hall, and D. Pappadopulo, Radiative PQ breaking and the Higgs boson mass, J. High Energy Phys. 06 (2015) 117.

[52] H. Georgi, D. B. Kaplan, and L. Randall, Manifesting the invisible axion at low-energies, Phys. Lett. **169B,** 73 (1986).

[53] F. Staub, SARAH, arXiv:0806.0538.

[54] F. Staub, From superpotential to model files for FeynArts and CalcHep/CompHep, Comput. Phys. Commun. **181,** 1077 (2010).

[55] F. Staub, Automatic calculation of supersymmetric renormalization group equations and self energies, Comput. Phys. Commun. **182,** 808 (2011).

[56] S. Davidson and J. R. Ellis, Basis independent measures of R-parity violation, Phys. Lett. B **390,** 210 (1997).

[57] H. K. Dreiner and M. Thormeier, Supersymmetric Froggatt-Nielsen models with baryon and lepton number violation, Phys. Rev. D **69,** 053002 (2004).

[58] H. K. Dreiner, H. E. Haber, and S. P. Martin, Two-component spinor techniques and Feynman rules for quantum field theory and supersymmetry, Phys. Rep. **494,** 1 (2010).

[59] Y. Grossman and H. E. Haber, Neutrino masses and sneutrino mixing in R-parity violating supersymmetry, arXiv:hep-ph/9906310.

[60] B. C. Allanach, A. Dedes, and H. K. Dreiner, Two loop supersymmetric renormalization group equations including R-parity violation and aspects of unification, Phys. Rev. D **60,** 056002 (1999); Erratum, Phys. Rev. D **86,** 039906(E) (2012).

[61] V. D. Barger, R. J. N. Phillips, and S. Sarkar, Remarks on the Karmen anomaly, Phys. Lett. B **352,** 365 (1995); Erratum, Phys. Lett. B **356,** 617(E) (1995).

[62] B. Mukhopadhyaya and S. Roy, Radiative decay of the lightest neutralino in an R-parity violating supersymmetric theory, Phys. Rev. D **60,** 115012 (1999).

[63] L. Lavoura, General formulae for $f_1 \rightarrow f_2\gamma$, Eur. Phys. J. C **29,** 191 (2003).

[64] S. Dawson, R-parity breaking in supersymmetric theories, Nucl. Phys. **B261,** 297 (1985).

[65] P. B. Pal and L. Wolfenstein, Radiative decays of massive neutrinos, Phys. Rev. D **25,** 766 (1982).

[66] M. Drewes *et al.*, A white paper on keV sterile neutrino dark matter, J. Cosmol. Astropart. Phys. 01 (2017) 025.

[67] CMS Collaboration, Search for selectrons and smuons at $\sqrt{s} = 13$ TeV, Report No. CMS-PAS-SUS-17-009, 2017.

[68] B. C. Allanach, A. Dedes, and H. K. Dreiner, Bounds on R-parity violating couplings at the weak scale and at the GUT scale, Phys. Rev. D **60,** 075014 (1999).

[69] P. Arias, D. Cadamuro, M. Goodsell, J. Jaeckel, J. Redondo, and A. Ringwald, Wispy cold dark matter, J. Cosmol. Astropart. Phys. 06 (**2012**) 013.

[70] R. Essig, E. Kuflik, S. D. McDermott, T. Volansky, and K. M. Zurek, Constraining light dark matter with diffuse X-ray and gamma-ray observations, J. High Energy Phys. 11 (2013) 193.

[71] O. Urban, N. Werner, S. W. Allen, A. Simionescu, J. S. Kaastra, and L. E. Strigari, A suzaku search for dark matter emission lines in the X-ray brightest galaxy clusters, Mon. Not. R. Astron. Soc. **451,** 2447 (2015).

[72] T. E. Jeltema and S. Profumo, Discovery of a 3.5 Kev line in the Galactic Centre and a critical look at the origin of the line across astronomical targets, Mon. Not. R. Astron. Soc. **450,** 2143 (2015).

[73] E. Bulbul, M. Markevitch, A. R. Foster, R. K. Smith, M. Loewenstein, and S. W. Randall, Comment on "Dark matter searches going bananas: The contribution of potassium (and chlorine) to the 3.5 keV line", arXiv:1409 .4143.

[74] A. Boyarsky, J. Franse, D. Iakubovskyi, and O. Ruchayskiy, Comment on the paper "Dark matter searches going bananas: The contribution of potassium (and chlorine) to the 3.5 keV line" by T. Jeltema and S. Profumo, arXiv:1408.4388.

[75] T. Jeltema and S. Profumo, Reply to two comments on "Dark matter searches going bananas the contribution of potassium (and chlorine) to the 3.5 keV line", arXiv:1411 .1759.

[76] E. Carlson, T. Jeltema, and S. Profumo, Where do the 3.5 keV photons come from? A morphological study of the Galactic Center and of Perseus, J. Cosmol. Astropart. Phys. 02 (2015) 009.

[77] O. Ruchayskiy, A. Boyarsky, D. Iakubovskyi, E. Bulbul, D. Eckert, J. Franse, D. Malyshev, M. Markevitch, and A. Neronov, Searching for decaying dark matter in deep XMM-Newton observation of the Draco Dwarf spheroidal, Mon. Not. R. Astron. Soc. **460,** 1390 (2016).

[78] T. E. Jeltema and S. Profumo, Deep Xmm observations of Draco rule out at the 99% confidence level a dark matter decay origin for the 3.5 keV line, Mon. Not. R. Astron. Soc. **458,** 3592 (2016).

[79] E. Bulbul, M. Markevitch, A. Foster, E. Miller, M. Bautz, M. Loewenstein, S. W. Randall, and R. K. Smith, Searching for the 3.5 keV Line in the stacked Suzaku observations of galaxy clusters, Astrophys. J. **831,** 55 (2016).

[80] J. J. Heckman, A. Tavanfar, and C. Vafa, Cosmology of F-theory GUTs, J. High Energy Phys. 04 (2010) 054.

[81] R. T. Co, F. D'Eramo, and L. J. Hall, Supersymmetric axion grand unified theories and their predictions, Phys. Rev. D **94,** 075001 (2016).

[82] R. T. Co, F. D'Eramo, L. J. Hall, and K. Harigaya, Saxion cosmology for thermalized gravitino dark matter, J. High Energy Phys. 07 (2017) 125.

[83] M. Kawasaki and K. Nakayama, Axions: Theory and cosmological role, Annu. Rev. Nucl. Part. Sci. **63,** 69 (2013).

[84] K. J. Bae, K. Choi, and S. H. Im, Effective interactions of axion supermultiplet and thermal production of axino dark matter, J. High Energy Phys. 08 (2011) 065.

[85] M. Kuster, G. Raffelt, and B. Beltran, Axions: Theory, cosmology, and experimental searches, Lect. Notes Phys. **741,** 1 (2008).

[86] M. Gorghetto, E. Hardy, and G. Villadoro, Axions from strings: The attractive solution, J. High Energy Phys. 07 (2018) 151.

[87] T. Hiramatsu, M. Kawasaki, T. Sekiguchi, M. Yamaguchi, and J. Yokoyama, Improved estimation of radiated axions from cosmological axionic strings, Phys. Rev. D **83,** 123531 (2011).

[88] L. Covi, H.-B. Kim, J. E. Kim, and L. Roszkowski, Axinos as dark matter, J. High Energy Phys. 05 (2001) 033.

[89] L. Covi and J. E. Kim, Axinos as dark matter particles, New J. Phys. **11,** 105003 (2009).

[90] A. Strumia, Thermal production of axino dark matter, J. High Energy Phys. 06 (**2010**) 036.

[91] K.-Y. Choi, L. Covi, J. E. Kim, and L. Roszkowski, Axino cold dark matter revisited, J. High Energy Phys. 04 (2012) 106.

[92] K.-Y. Choi, J. E. Kim, and L. Roszkowski, Review of axino dark matter, J. Korean Phys. Soc. **63,** 1685 (2013).

[93] R. T. Co, F. D'Eramo, and L. J. Hall, Gravitino or axino dark matter with reheat temperature as high as 10^{16} GeV, J. High Energy Phys. 03 (2017) 005.

[94] K. J. Bae, E. J. Chun, and S. H. Im, Cosmology of the DFSZ axino, J. Cosmol. Astropart. Phys. 03 (2012) 013.

[95] R. T. Co, F. D'Eramo, L. J. Hall, and D. Pappadopulo, Freeze-in dark matter with displaced signatures at colliders, J. Cosmol. Astropart. Phys. 12 (2015) 024.

[96] P. A. R. Ade *et al.* (Planck Collaboration), Planck 2015 results. XIII. Cosmological parameters, Astron. Astrophys. **594,** A13 (2016).

[97] K. Tamvakis and D. Wyler, Broken global symmetries in supersymmetric theories, Phys. Lett. **112B,** 451 (1982).

[98] T. Goto and M. Yamaguchi, Is axino dark matter possible in supergravity?, Phys. Lett. B **276,** 103 (1992).

[99] E. J. Chun, J. E. Kim, and H. P. Nilles, Axino mass, Phys. Lett. B **287,** 123 (1992).

[100] E. J. Chun and A. Lukas, Axino mass in supergravity models, Phys. Lett. B **357,** 43 (1995).

[101] P. Moxhay and K. Yamamoto, Peccei-Quinn symmetry breaking by radiative corrections in supergravity, Phys. Lett. **151B,** 363 (1985).

[102] J. E. Kim and M.-S. Seo, Mixing of axino and goldstino, and axino mass, Nucl. Phys. **B864,** 296 (2012).

[103] J. E. Kim and H. P. Nilles, The Mu problem and the strong *CP* problem, Phys. Lett. **138B,** 150 (1984).

[104] G. Honecker and W. Staessens, On axionic dark matter in type IIA string theory, Fortschr. Phys. **62,** 115 (2014).

[105] G. F. Giudice and R. Rattazzi, Theories with gauge mediated supersymmetry breaking, Phys. Rep. **322,** 419 (1999).

[106] L. J. Hall, J. D. Lykken, and S. Weinberg, Supergravity as the messenger of supersymmetry breaking, Phys. Rev. D **27,** 2359 (1983).

[107] A. H. Chamseddine, R. L. Arnowitt, and P. Nath, Locally Supersymmetric Grand Unification, Phys. Rev. Lett. **49,** 970 (1982).

[108] R. Barbieri, S. Ferrara, and C. A. Savoy, Gauge models with spontaneouslybroken local supersymmetry, Phys. Lett. **119B,** 343 (1982).

[109] T. Banks, M. Dine, and M. Graesser, Supersymmetry, axions and cosmology, Phys. Rev. D **68,** 075011 (2003).

[110] L. M. Carpenter, M. Dine, G. Festuccia, and L. Ubaldi, Axions in gauge mediation, Phys. Rev. D **80,** 125023 (2009).

[111] C. Cheung, G. Elor, and L. J. Hall, The cosmological axino problem, Phys. Rev. D **85,** 015008 (2012).

[112] S. Y. Choi, J. Kalinowski, G. A. Moortgat-Pick, and P. M. Zerwas, Analysis of the neutralino system in supersymmetric theories, Eur. Phys. J. C **22,** 563 (2001); Erratum, Eur. Phys. J. C **23,** 769(E) (2002).

[113] S. Y. Choi, D. J. Miller, and P. M. Zerwas, The neutralino sector of the next-to-minimal supersymmetric Standard Model, Nucl. Phys. **B711,** 83 (2005).